FEM simulation to clarify the Himalayan thrusts system

FEM simulation to clarify the Himalayan thrusts system

M. Farhad Howladar and Daigoro Hayashi

Simulation Tectonics Laboratory, Faculty of Science,
University of the Ryukyus, Okinawa 903-0213, Japan.

Abstract

Finite element method (FEM) is a general method of structural analysis in which a continuum or continuous structure is replaced by a finite number of elements interconnected at a finite number of nodal points. The method can be used to determine the displacements of the nodal points and stresses within the elements developed in two or three dimensional elastic or viscous structures of arbitrary geometrical and material properties. From this point of view, a 2D finite element method has been adopted to characterize the stress field and deformation pattern (mainly faults) in the Himalayan orogenic ranges. The Himalayas represent one of the few places on earth where continental crust is attempting to underthrust continental crust. As the Indian plate underthrusts beneath the Himalaya, it warps down in response to an advancing orogenic load and keeps the entire Himalayan mountain arc seismically active with which continuously influencing the stress field and structures in the regime. A series of elastic finite element models are presented to examine the state of stresses and faults on the models as well as within the incipient zones of major thrusts (MCT, MBT and MFT) after collision. Finally, the tectonic implementation of such simulated structures are drawn with combining the previously published geological, seismological and focal mechanism solution of faults data in the Himalayas.

The geologic profiles A, B, C and D of the central Himalayas which are used for the purpose under plane strain condition with elastic rheology. The elasticity of such model's layers considered with regards to the rock layer properties that there is a tendency, i.e. the older profiles might composed of the harder rocks and the older rock layers are the larger properties (e.g. density, Young's modulus and cohesion), whereas friction angle is lesser and Poisson's ratio is constant for all stages of models. The convergent rate of Indian plate has been considered 10 cm/a for profile A (40-20 Ma); 5 cm/a for B, C (20-10 Ma) and 2 cm/a for the present profile A (0 Ma). The results show that the compressive stress and the thrust fault dominant over the whole period after collision.

Some interesting findings of the numerical models are: (1) simulated state of stresses is compressive in nature, where σ_1 oriented horizontally, is resulting the thrust faults of the

Received: July 6, 2006

models; (2) state of stresses and intensity of failure elements (faults) are mainly controlled by the model geometry, boundary condition and layers properties; (3) displacement boundary conditions are sensitive for both of the stresses magnitude and faults whereas layer properties are mainly sensitive to the fault development; (4) thrust faults are frequently formed within the low-grade rocks layers than in the high-grade rock layers; (5) thrust faults are localized within the whole area of incipient zones of MCT (40-20 Ma), MBT (20-10 Ma) and MFT (10-0 Ma) as well as along the initial boundaries of these future thrusts; (6) faulting tendency increases in the younger rock sequences of the profiles with their propagation southward; (7) good agreement of simulated stress and thrust faults with the existed geologic records in this compressional regime; (8) numerically developed faults since 40 Ma to present are direct evidences to the transformation of active subduction of Indian continental crust from north to south; (9) localization of thrust faults along the MCT at primary stage of post collision then MBT (20-10 Ma) and finally along the MFT (10-0 Ma) suggesting that the age of initiation of these thrusts becomes from MCT to MFT, with the MCT as the oldest and MFT as the youngest; (10) intense development of fault around the major thrusts (MBT an MFT) and along the frontal part of Himalayas indicating that these areas are tectonically active which support the present neotectonics in the Himalayas.

The distribution of stress trends and faults calculated in the models are compared with the previously published geological data, earthquakes focal mechanism solutions of faults and active faults analysis data in the Himalayas. Comparison shows the close similarities between the simulated results and the aforesaid published data. Finally on the basis of the numerical modeling results and summary of former geological and geophysical researches, a preliminary hypothesis is proposed on the structural and tectonic development of the Himalayan orogeny, where especial attention has been paid for examining the earlier development stage of stress state and fault in the incipient zones of the future thrusts MCT, MBT and MFT as well as the present stage. The compressive stress and thrust faults within the incipient zones might be the responsible for the earlier development stage of MCT (40 Ma), MBT (20 Ma) and MFT (10 Ma) which may paved the way for posing that the MCT is the oldest and MFT is the youngest thrusts in the Himalayas and they are propagating southward from the initiation time. Thus It is very convenient to state that the continuous propagation of such thrusts might have greatly influenced the tectonics and structures in this compressoinal mountain belt. Presently, around the frontal part of the Himalayas might be more active due to development of large numbers simulated faults which is also responsible for the neotectonic activity in the regimes.

Introduction

The Himalayan mountain ranges were formed by the collision of Indian plate with the Asian continent about 50 Ma (Johnson, 2002). This continent-continent convergence has lead to high mountain chain along the convergence line (Fig. 1) while the Indian Plate subducts under the Asian continent. As a result of the convergent plate motion numerous tectonic structures were formed in the Himalayas (Armbuster et al., 1978; Lyon-Caen and Molnar, 1983; Upreti, 1999; Lave and Avouac, 2000; Johnson, 2002). There are some major tectonic structures in the Himalayas that are the Main Central Thrust (MCT), the Main Boundary Thrust (MBT), Main Frontal Thrust (MFT) and Main Himalayan Thrust (MHT). These thrusts can be traced almost throughout the entire Himalayan range. The historical earthquakes in Himalayas are mostly occur along these thrust zones (Seeber et al., 1981). From these features, it is obvious that these structures might have an important role to the tectonic development of the Himalayan mountain ranges.

Thus, the Himalayan mountain ranges provide a spectacular natural laboratory for the study of continental collision in the uplifted section of crust. Pioneer geological investigations have delineated the fundamental tectonic framework of the Himalayan territory. Based on the field-laboratory experimental studies, numerical modeling of various aspects for collision tectonics has been achieved by many earth's scientists (e.g. the collision-indentation model of Indian craton by Molnar and Tapponnier, 1975; the thermal relaxation model of England and Thompson, 1984; numerical simulation model for the uplift of the Tibetan plateau by Hayashi, 1987; Himalayan geologic evolutionary model of Yin et al., 1994; the wedge extrusion of high-grade metamorphic rocks by Chemenda et

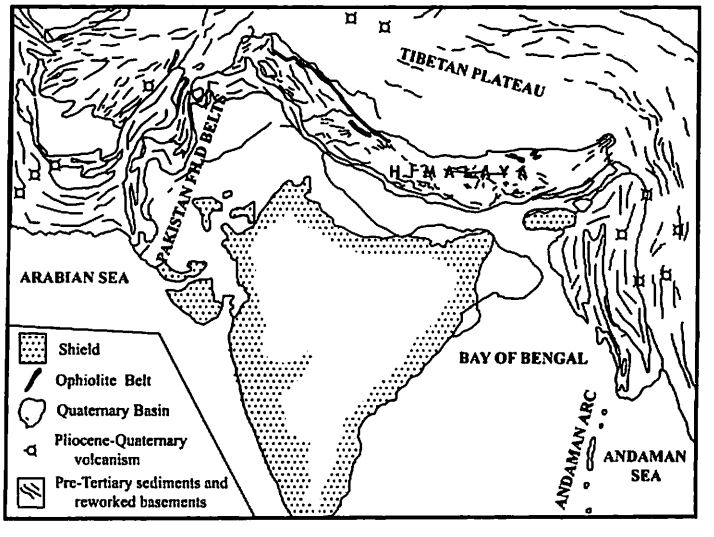

Fig.1. Regional tectonic setting of the Himalayan arc at the northern margin of the Indian subcontinent modified after Gansser (1964) and Seebar et al. (1981).

al., 1995; the 3D deformation and stress model in the Himalaya by Sato et al., 1996; the thermo-mechanical experimental modeling of continental subduction by Chemenda et al., 2000 and Yin and Harrison 2000; the elastic wedge model of Himalayan orogeny by Shanker et al. 2002; the elastic plain strain model for the development of Himalayan fault system and major thrusts by Howladar and Hayashi, 2003 and 2004; numerical fault modeling along the Himalayan profiles by Chamlagain and Hayashi, 2004). Nevertheless, the orogenic processes of the Himalayan mountain range are not yet fully understood. Therefore, it is essential to improve knowledge of the structural characteristics and tectonics along the geologic as well as structural cross section of the Himalayan region

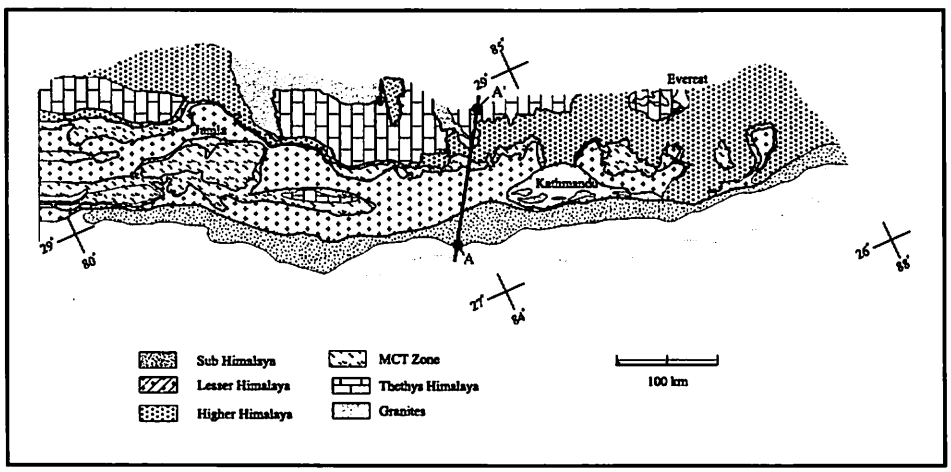

Fig.2. Geological map of Nepal (Kizaki and Hayashi, 1984). A-A' line shows the model Profiles.

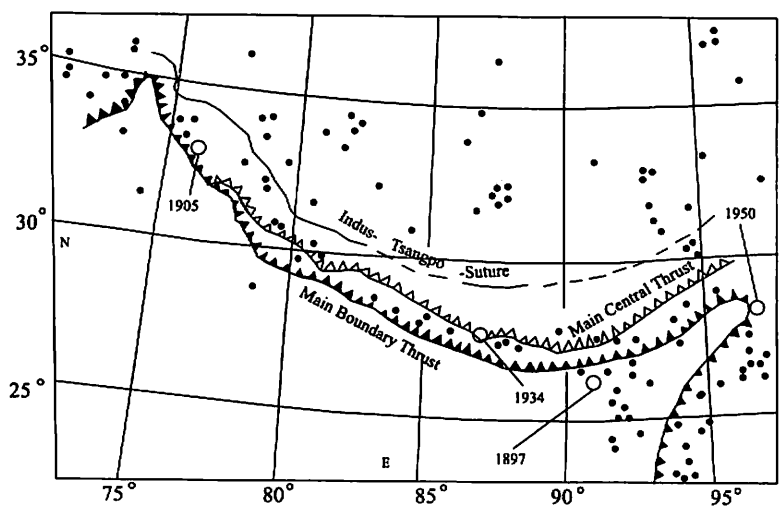

Fig.3. The characteristics of shallow focus seismicity map of the Himalayan region modified after Molnar et al. (1977).

Records of historical convergent rate after cllision

Time span (Ma)	convergent rate (cm/ a)
40-20	10
20-10	5
10-0	5
0	2

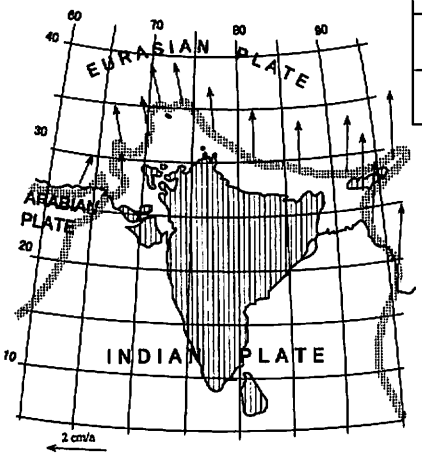

Fig.4. The relative convergent motion between the Indian and Eurasian plates modified after Minster and Jordan (1978) and Nakata et al. (1990).

after collision.

From these viewpoints, we choose a series of geologic cross profiles from the central part of Himalayas which consists of four model profiles. The four models are: model A (40 Ma), model B (20 Ma), model C (10 Ma) and model D (present). The model profiles have been modified and reconstructed with natural scale from Johnson (2002) and Howladar and Hayashi (2004), where the major structures are MCT, MBT and MFT which were primarily created from their incipient zones at 40, 20 and 10 Ma, respectively. We treat the incipient zone of these thrusts as the area to explore their early developing stress state and element failure (fault).

The aim of the present study is to examine the development of major thrusts and states of stress in Himalayas. Therefore, we primarily calculate stress distribution and faults in all stages of models as well as within the incipient zone of the future thrusts (MCT, MBT and MFT) considering elastic rheology and sequential convergent rate of Indian sub-plate after collision by finite element method with Mohr Coulomb failure criterion. Then the simulated results are compared with the previous studies. Finally combining all of these data, a preliminary model is proposed on the successive development of major structures (MCT, MBT and MFT) and discussed their associated tectonics.

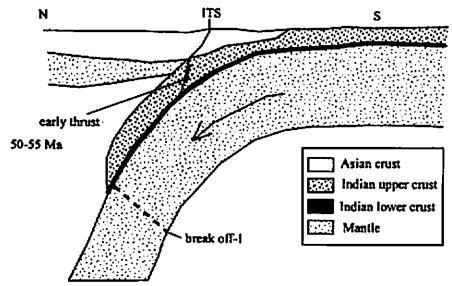

(A). Initial stage of collision: subduction of Indian continental crust at 50-55 Ma.

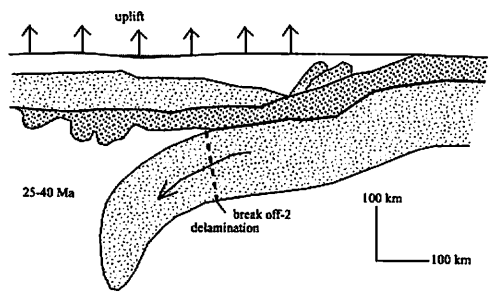

(B). Rapid uplift of the subducted crustal sheet to a few to several tens of killometers depth. Break-off of Indian mantle with the attached subducted ocenic lithosphere at 25-40 Ma.

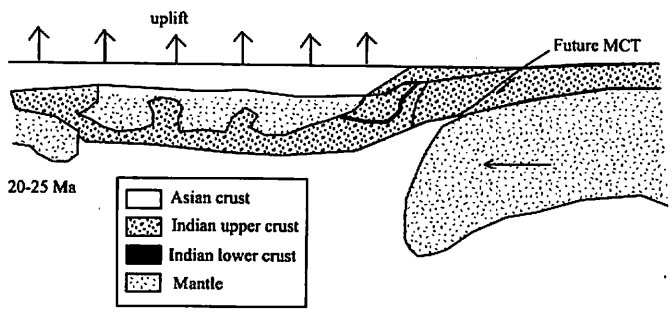

(C) Formation of major crustal thrust: failure of the indian crust in front of orogen and the formation of Main Central Thrust (MCT) at 20-25 Ma.

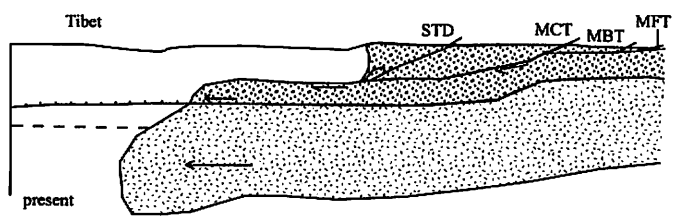

(D) Present stage of Himalaya with Major continental structures (MCT, MBT, MFT and STDS).

Fig.5. Tectonic and structural development of Himalaya-Tibet orogernic system after Chemenda et al, 2000.

Geologic divisions and major structures

Commonly Himalayas can be divided, from north to south into the four major geologic divisions which are separated one from another by the intra-continental thrusts (Fig. 2). The geologic divisions and major thrusts are: Tethys Himalaya (TH), Higher Himalaya (HH), Lesser Himalaya (LH), Sub-Himalaya (SH) and Main Central Thrust (MCT), Main Boundary Thrust (MBT), Main Frontal Thrust (MFT), respectively. According to Lyon-Caen and Molnar (1983); Kaneko (1997) and Johnson (2002), the Indus Tsangpo Suture (ITS), Tibetan oceanic crust (TOC), Base of Indian continental Crust (BICC) and incipient zones of MCT, MBT ant MFT have been considered for the present numerical model profiles (Fig. 7). Each of the divisions is characterized by its own

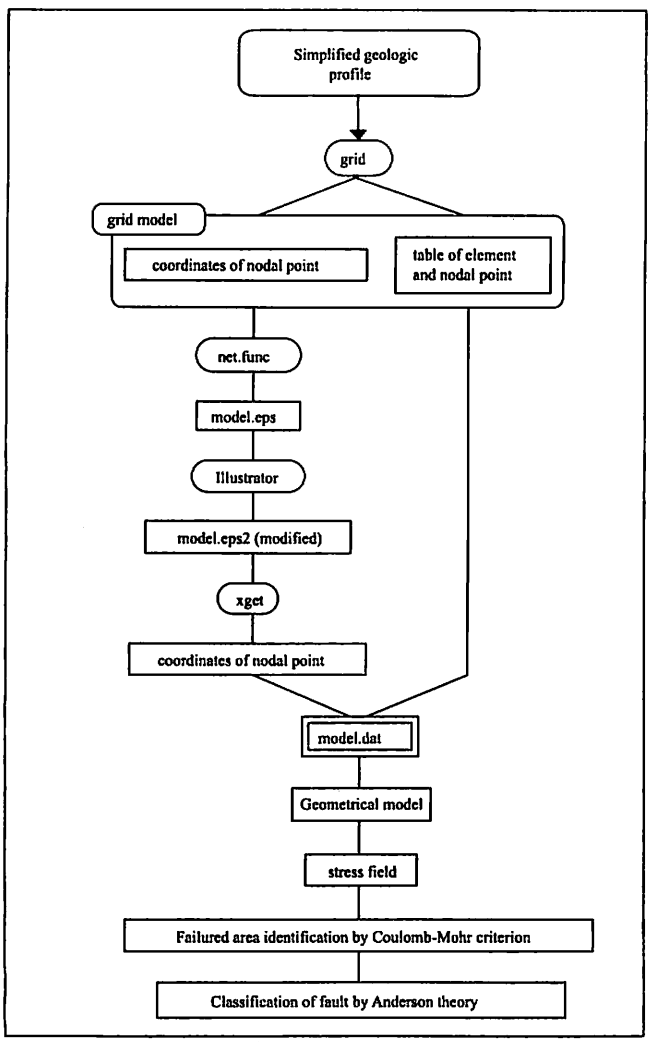

Fig.6. Generalized flow chart to construct the finite element models for stress and fault Calculation.

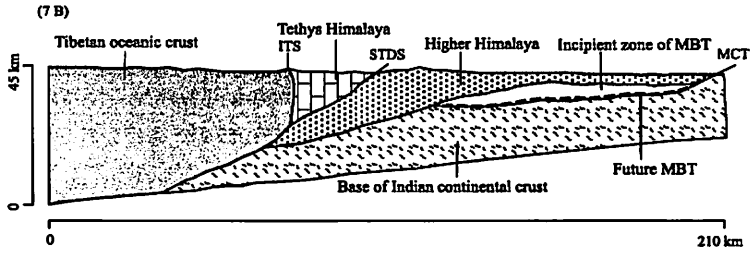

Fig.7 A. Balanced geologic cross profile A at 40 Ma of the central Himalaya, rearranged after Johnson (2002). MCT= Main Central Thrust, STDS= South Tibetan Detachment System and ITS= Indus Tsangpo Suture.

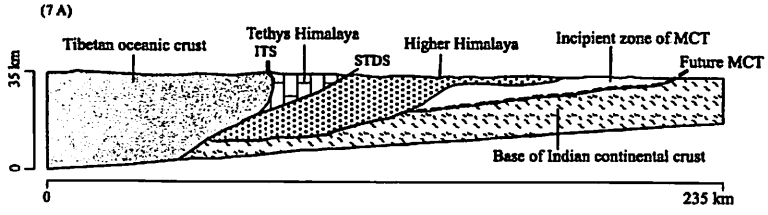

Fig.7 B. Balanced geologic cross profile B at 20 Ma of the central Himalaya, rearranged after Johnson (2002). MCT= Main Central Thrust, MBT= Main Boundary Thrust, STDS= South Tibetan Detachment System and ITS= Indus Tsangpo Suture.

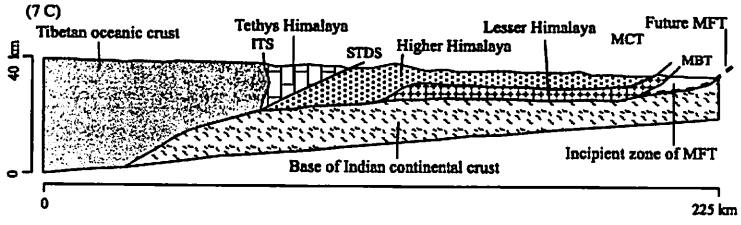

Fig.7 C. Balanced geologic cross profile C at 10 Ma of the central Himalaya, rearranged after Johnson (2002). MCT= Main Central Thrust, MBT= Main Boundary Thrust, STDS= South Tibetan Detachment System and ITS= Indus Tsangpo Suture.

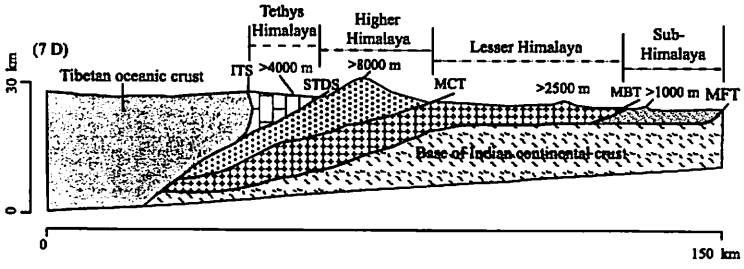

Fig.7 D. Balanced geologic cross profile D at 0 (present) Ma of the central Himalaya, rearranged after Johnson (2002). MCT= Main Central Thrust, MBT= Main Boundary Thrust, MFT= Main Frontal Thrust, STDS=South Tibetan Detachment System and ITS= Indus Tsangpo Suture.

lithology, tectonics, structures and geologic history. All of these mentioned above geologic zones, lithology, structures and their topographic height are shown in Table 1.

Geologic divisions

Tibetan Oceanic Crust

Tibetan oceanic crust is the northern part of the Himalayan profile models (Lyon-

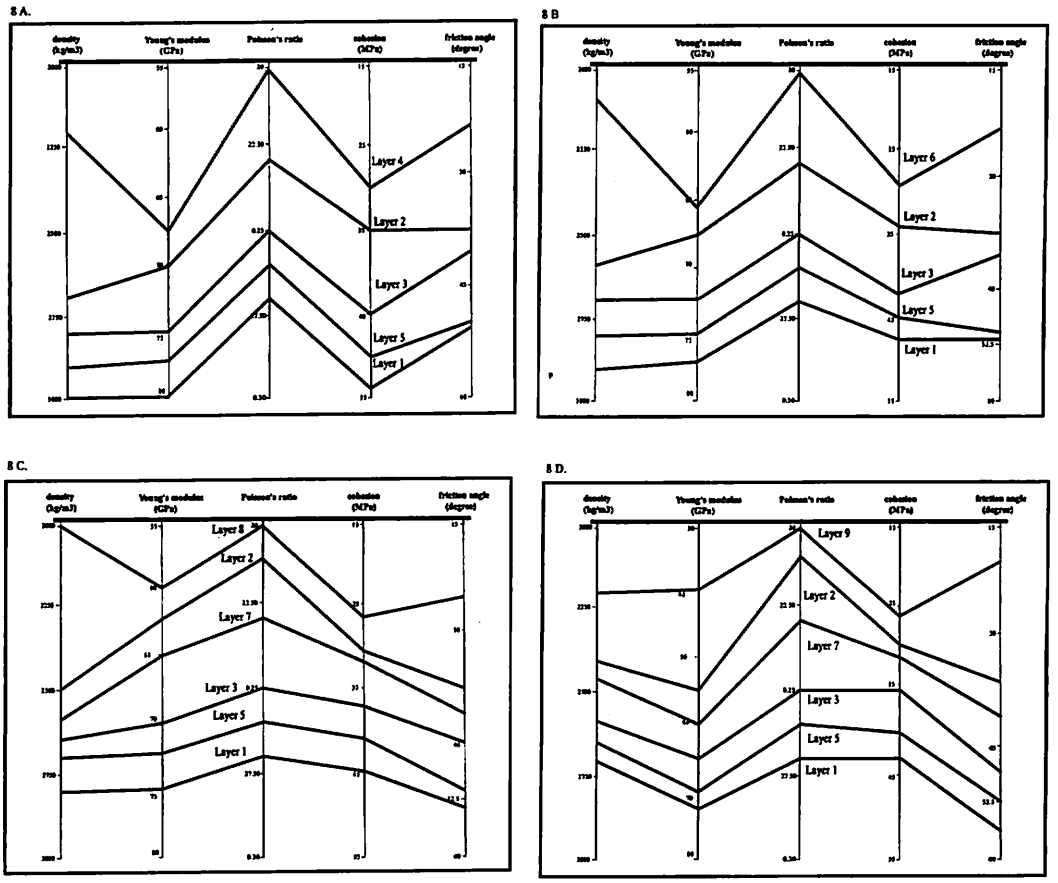

Fig.8 A. Graphical illustration of physical parameters of different layers of model A in central Nepal. 1= Tibetan Oceanic Crust, 2=Tethys Himalaya, 3=Higher Himalaya, 4= Incipient Zone of Main Central Thrust, 5= Base of Indian Continental Crust.

Fig.8 B. Graphical illustration of physical parameters of different layers of model B in central Nepal. 1= Tibetan Oceanic Crust, 2=Tethys Himalaya, 3=Higher Himalaya, 5=Base of Indian Continental Crust, 6= Incipient Zone of Main Boundary Thrust.

Fig.8 C. Graphical illustration of physical parameters of different layers of model C in central Nepal. 1= Tibetan Oceanic Crust, 2=Tethys Himalaya, 3= Higher Himalaya, 5=Base of Indian Continental Crust, 7= Lesser Himalaya, 8= Incipient Zone of Main Frontal Thrust.

Fig.8 D. Graphical illustration of physical parameters of different layers of model D in central Nepal. 1= Tibetan Oceanic Crust, 2=Tethys Himalaya, 3=Higher Himalaya, 5=Base of Indian Continental Crust, 7= Lesser Himalaya, 9=Sub-Himalaya.....68

Table 1. Generalized tectonic elements and stratigraphic zones of Himalayas.

layer nos.	major structures, tectonic divisions and their physical characters			altitudes
	Indus-Tsangpo suture			
2	Tethys Himalayas	Tibetan Tethys Group	Mainly lower Paleozoic to Mesozoic clastic and calcareous sediments	2500-4500m
	South Tibetan Detachment System			
3	Higher Himalayas	Himalayan Gneiss Group	Rejuvenated Precambrian basement, mostly polymetmorphosed and migmatized at the Alpine stage by the intrusion of tourmaline granites	5000-8800m
	Main Central Thrust			
7	Lesser Himalayas	Midland Group	Mainly Eocambrian clastic Sediments with limestone and quartzite, mostly altered to phyllite and metasandstone	200-2600m
	Main Boundary Thrust			
9	Sub-Himalayas	Churia (Siwalik) Group	Tertiary to Quaternary molasses sediments	200-1000m
	Main Frontal Thrust			
	Indian Gangetic Plain	Siwalik Group - Younger	Recent sediments	100-200m

Table 2. Post-collisional convergent rate and displacement between Indian and Eurasian plate.

models	convergent rate (cm/ a)	time span (Ma)	convergent displacement	stress and fault
A	10	40-20	2000 m (for 20 ka)	MCT
B	5	20-10	1000 m (for 20 ka)	MBT
C	5	10-0	1000 m (for 20 ka)	MFT
D	2	0 (present)	400 m (for 20 ka)	present stress and fault

Table 3. Geotectonic divisions and their lithological characteristics of models A, B, C and D.

Rock layer	Corresponding layer nos.	Considered rock species
Tibetan oceanic crust	1	Basalt
Tethys Himalaya	2	Limestone and sandstone
Higher Himalaya	3	Gneiss, schist and granite
Lesser Himalaya	7	Phyllite, slate, limestone and sandstone
Incipient zone of MCT and MBT	4 and 6	Meta-sedimentary rocks
Incipient zone of MFT	8	Clastic sedimentary rocks
Sub-Himalaya	9	Sandstone and siltstone
Base of continental crust	5	Crystalline gneiss and granite

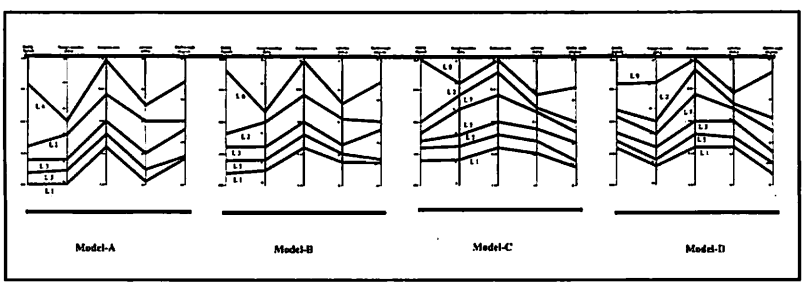

Fig.9. Comparison of layer parameters of models A, B, C and D. Here 1, 2, 3, 5, 7, 9, 4, 6 and 8= Tibetan oceanic crust, Tethys Himalaya, Higher Himalaya, Indian continental crust, Lesser Himalaya, Sub-Himalaya, Incipient Zones of MCT, MBT and MFT, respectively.

Caen and Molnar, 1983; Chemenda et al., 1995; Johnson, 2002). This zone is separated from the Tethys Himalaya by the Indus Tsangpo Suture. One important factor distinguishing oceanic lithosphere from continental lithosphere is that the former is significantly younger than the latter. The great difference between the ages of continental and oceanic lithosphere may be explained by the fact that subduction continually recycles oceanic lithosphere and so never has the opportunity to accumulate and age for billions of years. Additionally, there are fossils of sea creatures that are much older than the ocean floor, thus supporting the idea that oceanic crust is being destroyed along subduction zones. Oceanic lithosphere is primarily basaltic in composition and this is essentially due to its creation along oceanic ridges.

Table 4 A. Rock layers properties of central Himalayan model A.

layer nos.	rock layers	density (kg/m^3)	Poisson's ratio	Young's modulus (GPa)	cohesion (MPa)	friction angle (degree)
1	Tibetan oceanic crust	3000	0.27	80.0	52.00	51.0
2	Tethys Himalaya	2700	0.23	70.0	35.00	37.0
3	Higher Himalaya	2800	0.25	75.0	45.00	40.0
4	Incipient zone of MCT	2200	0.20	67.5	30.00	23.0
5	Base of continental crust	2900	0.26	77.5	50.00	50.50

Table 4 B. Rock layers properties of central Himalayan model B.

layer nos.	rock layer	density (kg/m^3)	Poisson's ratio	Young's modulus (GPa)	cohesion (MPa)	friction angle (degree)
1	Tibetan oceanic crust	2900	0.27	77.5	47.50	52.0
2	Tethys Himalaya	2600	0.23	67.5	34.00	40.5
3	Higher Himalaya	2700	0.25	72.5	42.50	42.0
6	Incipient zone of MBT	2100	0.20	65.5	29.00	24.0
5	Base of continental crust	2800	0.26	75.0	45.00	51.0

Table 4 C Rock layers properties of central Himalayan model C.

layer nos.	rock layer	density (kg/m^3)	Poisson's ratio	Young's modulus (GPa)	cohesion (MPa)	friction angle (degree)
1	Tibetan oceanic crust	2800	0.27	75.0	45.00	53.0
2	Tethys Himalaya	2600	0.23	65.0	32.00	42.0
3	Higher Himalaya	2650	0.25	70.0	37.00	45.5
7	Lesser Himalaya	2500	0.21	62.0	31.00	37.0
8	Incipient zone of MFT	2000	0.20	60.0	27.00	25.0
5	Base of continental crust	2700	0.26	72.0	42.00	52.0

Table 4 D Rock layers properties of central Himalayan model D.

layer nos.	rock layer	density (kg/m^3)	Poisson's ratio	Young's modulus (GPa)	cohesion (MPa)	friction angle (degree)
1	Tibetan oceanic crust	2700	0.27	72.5	43.00	55.0
2	Tethys Himalaya	2450	0.23	60.0	31.00	43.5
3	Higher Himalaya	2600	0.25	65.0	35.00	47.0
7	Lesser Himalaya	2400	0.21	55.0	29.00	36.0
9	Sub-Himalaya	2200	0.20	40.0	26.00	20.0
5	Base of continental crust	2650	0.26	70.0	40.00	52.5

Table 5. Distribution of some representative values of σ_1 and τ_{max} in model A, B, C and D.

models	maximum principal stress (σ_1) (MPa)			maximum shearing stress (τ_{max}) (MPa)		
	depth limit			depth limit		
	shallowest	middle	deepest	shallowest	middle	deepest
A	100	400-500	800	300	200	150
B	100	400	800	180	40-60	120-140
C	50	400-500	700	120	20-60	90-100
D	50	250-300	400	90	10-30	80

Sub-Himalayan zone

This foreland zone consists of clastic sediments that were produced by the uplift and subsequent erosion of the Himalayas and deposited by rivers. These rocks have been folded and faulted to produce the Siwalik Hills that are at the foot of the great mountains. According to Hagen (1969), the Lower, Middle and Upper Siwalik is available in this region. The Middle Siwalik is prominent in the Nepalese Sub-Himalayas. Lower part of this group consists of brick colored fine to medium grained sandstone and contains some intercalations of muscovite bearing coarse-grained sandstone. The middle part is made up of fine to medium grained calcareous sandstone and of fine to medium grained brick colored sandstone in the upper portion. The Upper part is largely composed of conglomerate. Predominantly pale schistose quartzites, purple and white quartzites, dark hyalites, arkoses, purple and dark pebbly quartzites, salty brown sandstones and tourmaline (Gansser et al., 1964 and Arita et al., 1984). Siwalik in the Karnali-Bheri region contains sandstone, mudstone, conglomerate and limestone (Fuchs and Frank, 1970).

Sub-Himalayan rocks have been overthrust by the Lesser Himalayas along the Main Boundary Thrust. This steep thrust flattens with depth, developed during the Pliocene time and has been shown as active through the Pliestocene (Ni, et al., 1984). In turn, the Sub-Himalayas are bounded by a thrust fault to the south and are forced over sediments on the Indian plate. This fault system is called the Himalayan Frontal Thrust (Sorkhabi and Macfarlane, 1999).

Lesser Himalayan zone

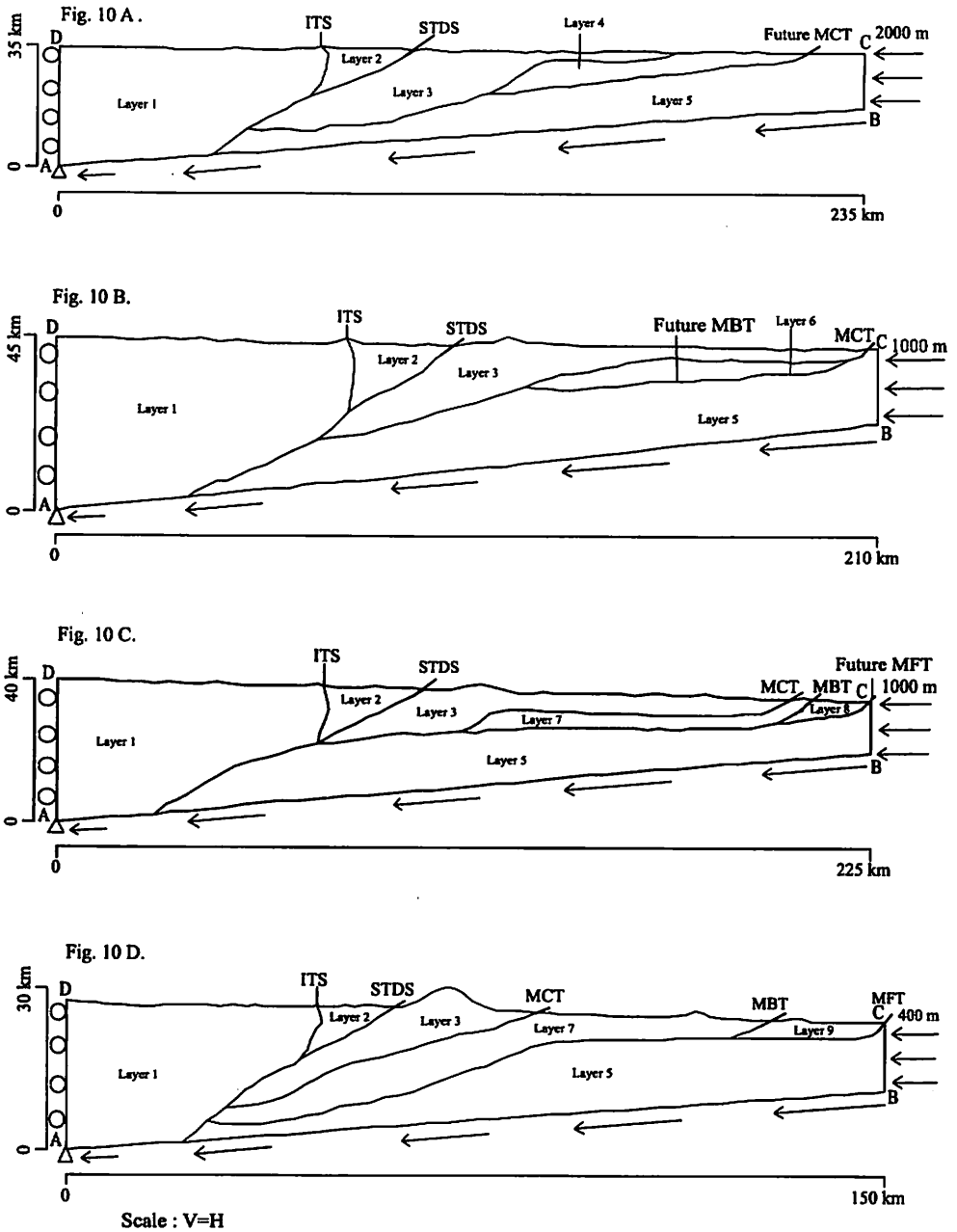

Fig.10. Geometry and boundary constraints of finite element models A, B, C and D. Different layers and rheologies (Young's modulus, Poisson's ratio, density, cohesion and angle of internal friction listed in Table 1). Open triangle= fixed point; open circles = fixed only horizontal direction, arrows= imposed displacement. Simulated models are represented by six or seven structural units as to their regional tectonic setting which are marked by the Roman characters 1, 2, 3, 4, 5, 6, 7, 8 and 9. Here 1, 2, 3, 5, 7, 9, 4, 6 and 8= Tibetan oceanic crust, Tethys Himalaya, Higher Himalaya, Indian continental crust, Lesser Himalaya, Sub-Himalaya, Incipient Zones of MCT, MBT and MFT, respectively.

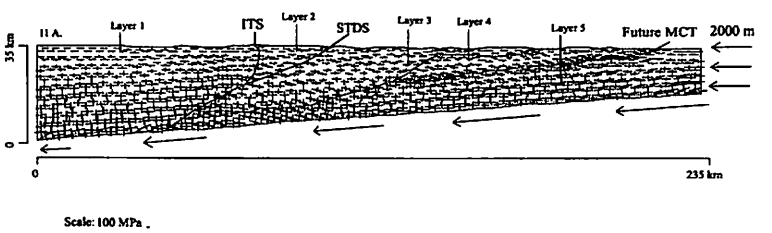

Fig.11 A. Distribution of principal stress of model A under 2000 m convergence displacement boundary condition where black color reflects compressive and red tensile stress. Layer 1= Tibetan oceanic crust, Layer 2= Tethys Himalay, layer 3= Higher Himalaya, layer 4= Incipient zone of MCT and layer 5= Base of Indian Continental crust.

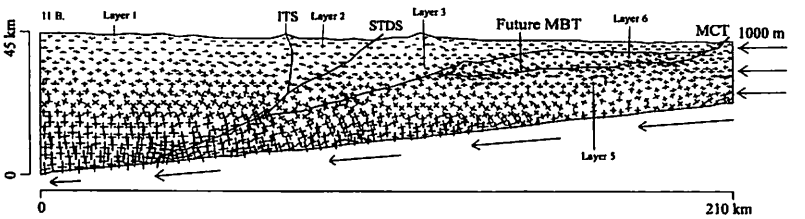

Fig.11 B. Distribution of principal stress of model B under 1000 m convergence displacement boundary condition where black color reflects compressive and red tensile stress. Layer 1= Tibetan oceanic crust, Layer 2= Tethys Himalay, layer 3= Higher Himalaya, layer 6= Incipient zone of MBT and layer 5= Base of Indian Continental crust.

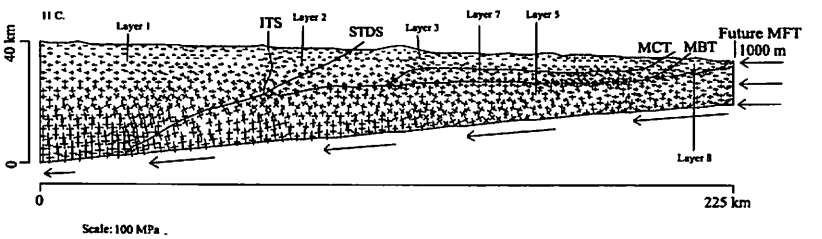

Fig.11 C. Distribution of principal stress of model C under 1000 m convergence displacement boundary condition where black color reflects compressive and red tensile stress. Layer 1, 2, 3 and 5 are same as previous figure. Here the layer 7 and 8= Lesser Himalaya and Incipient zone of MFT, respectively.

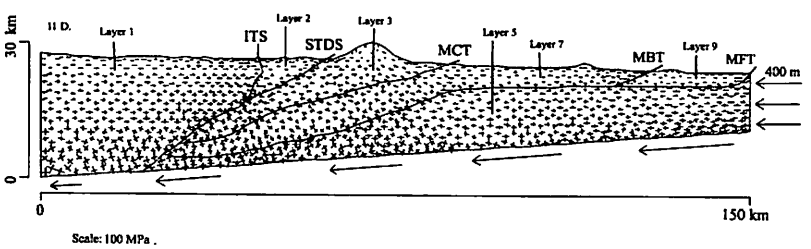

Fig.11 D. Distribution of principal stress of model D under 400 m convergence displacement boundary condition where black color reflects compressive and red tensile stress. Layer 1, 2, 3, 5 and 7 are same as previous figure and here the layer 9= Sub-Himalaya.

The Lesser Himalayan zone is bounded the Main Central Thrust (MCT; Table 1) in the north and Main Boundary Thrust (MBT) to the south (Fig. 2). Unlike the Higher Himalayas, the Lesser Himalaya only experienced up to greenschist facies metamorphism. The rock types present here are also different and they are belonging to the Midland metasediments group. Midland meta-sediments sequence presents two types of lithofacies that are observed separately in the north and south part of the Nepal. Southern facies is composed of limestone, slate and phyllite and northern facies consists of slate, limestone and siliceous sandstone and with some schist (Hayashi et al., 1984). This group in the Jajarkot area comprises mainly of garnet-mica, chlorite phyllite schist, black phyllite, crystalline limestone, blastomylonitic augen gneiss, limestone, dolomite and calcareous sandstone (Arita et al., 1984).

Rock units here also show a series of anticlines and synclines that are in many cases quite sheared. Fossils have been documented in this zone, but they do not occur at the same frequency as Tehtyan zone fossils.

Higher Himalayan zone

The Higher Himalaya (Fig. 2) also known as the Central Crystalline zone, comprised of deformed metamorphic rocks and mark the axis of orogenic uplift. Mica schist, quartzite, paragneiss, migmatite, and leucogranite bodies characterize this uppermost Himalayan zone. They represent a multiphase deformation event, the first being Barrovian type, or normal geothermal gradient conditions. There was then a shift to Buchan-type metamorphism, low pressure and high temperature conditions, with temperatures greatly exceeding normal gradient temperatures (Sorkhabi and Macfarlane, 1999). Corresponding minerals assemblages are dominated by biotite to sillimanite, representing greenschist to amphibolite facies deformation. Deformation seems to have occurred in a north to south direction and is associated with the Main Central Thrust Fault (MCT), which brings the Higher Himalayas on top of the lower Himalayas (Sorkhabi and Macfarlane, 1999). Initially, it was thought that approximately 350 km of shortening had occurred in the Greater Himalayan sequence of rocks.

Tethys Himalayan zone

The Tethyan Himalayas are located to the south of the ITSZ. The belt has been extending from Kashmir to Nepal. Spiti valley in Himachal Pradesh and Kashmir where have seen a continuous succession from Precambrian to Mesozoic ages. They consist of thick, 10-17 km, marine sediments that were deposited on the continental shelf and slope of the Indian continent. This occurred as India was drifting but still in the southern hemisphere (Verma, 1997). Sediments are largely unmetamorphosed, which has made for excellent preservation of fossils and occur in synclinorium-type basins. Some however, have experienced greenschist facies deformation (Windley, 1995). Fossils occur in this east-west zone within strata that are very clearly known. The large variety of size and distribution of fauna suggests that life was flourishing in this area before the orogen.

Such success in biological diversity is accounted for by the relatively stationary position of the Tehthyan Zone between mid-Proterozoic and Eocene time. Episodic formation of land barriers enabled life to grow and diversify (Sorkhabi and Macfarlane, 1999).

Basement of continental crust

The basement rocks are distributed many places over the Nepal Himalaya as exposed or unexposed formation. Tethyan Himalayas are found mixed with the granitic rocks. The oldest recognized unit in Spiti is the Vaikrita Group which is overlain by the Haimanta Group. They consist of mica schist, phyllite and quartzite. The oldest rocks of the Kashmir Tethyan basin belong to the Salkhala Group. The rocks are slate, phyllite, schist, marble and quartzite. The lower part of this group is often mixed with granitic rocks. The Salkhala Group is overlain by Dogra Slate of Late Precambrian age. The Upper Precambrian, of an elongated and narrow intracontinental sea between the Indian continent and the Cimmerian Superterrane is documented by the sedimentary series of the Phe Formation. The sediments of this 5000 to 10,000 metres thick formation are mainly derived from the erosion of the relief fringing this trough to the north (Fuchs and Linner, 1995).

Incipient Zones of Major Thrusts (MCT, MBT and MFT)

In the present simulation, the incipient zone of major thrusts are considered based on the balanced geologic profiles of Lyon-Caen and Molnar (1983); Johnson (2002). In these profiles, they marked the early developing state of future thrusts by dashed line and mature stage by solid line (Fig. 7). Therefore the early to mature stage boundaries are defined in terms of incipient development zones of such thrusts. The geometrical position of MCT and MBT zones are below the Hihger Himalaya which are equivalent to the lesser Himalayan sequences. The position of MFT zone is the southern part of lesser Himalaya and equivalent to Sub-Himalaya. Thus the meta-sedimentary and clastic sedimentary rocks are considered for these zones, respectively.

Major structure

Indus Tsangpo Suture (ITS)

This structure marks the limit between the Indian Plate and the Eurasian plate. It is along the Indus Suture zone that the Indian plate was subducted below Eurasia. Remains of oceanic crust and island arc, mixed with flysch and molasse deposits, can be found within the ITSZ as well as in the Spontang Klippe (Dèzes, 1999).

South Tibetan Detachment System (STDS)

The South Tibetan Detachment System also called North Himalayan Shear Zone (NHSZ), represents a major system of north-dipping structural detachments at the boundary between the High Himalayan Crystalline Sequence and the Tethys Himalaya (Fig. 2). This structure was first identified by Burg and Chen (1984). A detailed analysis of the STDS was made by Burchfiel et al. (1992). Deformation along this structure was

accommodated either by dextral strike-slip or by extensional shearing. Unlike the MCT, the STDS is not a continuous structure along the entire Himalayan belt.

Main Central Thrust (MCT)

This thrust described by Gansser (1964) when he noted a contact between terrigenous carbonate rocks and thick overlying metamorphic rocks, mica schists and gneiss (Sinha, 1987). The Main Central Thrust marks the boundary between the Higher and Lesser Himalayan mountain (Fig. 2). It is a longitudinal thrust fault, and in many places is marked by a several kilometer thick zone of deformed rocks with varying degrees of shearing and imbrication (Sorkhabi and Macfarlane, 1999). Mylonitization and retrograde metamorphic assemblages also occur here. The MCT is the actual suture between Gondwanaland (India) and the Proto-Tehtys microcontinent to the north (Spikantia, 1987). Movement along the fault has brought crystalline rock from the Higher Himalayan zone on top of Lesser Paleozoic sediments in the form of klippen in synclines (Windley, 1995). These units are called the Outer Crystallines. Outer crystalline rocks, garnet and kyanite-bearing, were exposed by slip along the MCT followed by uplift and erosion of 10 km of overlying rock (Molnar, 1990).

Main Boundary Thrust (MBT)

This structure separates the metapsammitic schists and phyllites of the Lesser Himalaya from the conglomerates and sandstones of the Sub-Himalaya (Arita, et al., 1984). The SW-directed movements associated with this structure are characterized by brittle deformation.

Main Frontal Thrust (MFT)

The Sub-Himalayas are bounded by a thrust fault to the south and are forced over sediments on the Indian plate. This type of fault is known as the Himalayan Frontal Thrust (Dèzes, 1999). The MFT is along this still active structure that the Sub-Himalaya is thrust towards the SW over the Quaternary fluvial deposits of the Indian plains.

Geophysical information

Seismic characteristics and earthquakes in the Himalayas

The structure, topography and seismicity are quite uniform along the Himalayan front. The most prominent seismic feature is a narrow earthquakes belt where all available fault-plane solutions indicate thrusting and this belt can easily identify along the entire Himalayas (Seeber et al., 1981). Himalayan mountain range and its adjoining area constitutes one of the most seismically active regions of the world. Four earthquakes with magnitudes greater than 8 occurred since 1897 and all appear to be related to mountain building processes in the Himalayas. The earthquakes epicenters fall near the trace of the Main Central Thrust and not near the Main Boundary Thrust. From this observation it is tempting to conclude that the MCT is active but not the MBT. However, one considers that the MBT dips gently to the north or northeast (Gansser, 1964), and that

earthquakes occur at finite depth, it seems more reasonable to conclude that along most of the Himalayas, the activity is associated with the MBF and the zone surrounding it. The seismicity at the both ends of the Himalayas appear to be more complicated with diffuse zone south of the main ranges.

The southward migration of thrust faults may result in part from the buoyancy of continental crust. In the east, seismicity is distributed over the Shillong plateau and it's margins (Fig. 3). Jacob et al. (1976) and Armbuster et al. (1978) considered both the Main Central Thrust and the Main Boundary Thrust to be active in the northwest meanwhile the tectonics of this part of the Himalayas is possibly too abstruse than to the southeast. From these pictures, Jacob et al. (1976) and Armbuster et al. (1978) assumed that the seismicity along the entire range is not restricted to a single narrow fault zone. The level of seismic activity along the Indus-Tsangpo suture zone is very low. The lack of seismicity along the suture zone indicates that this region is relatively rigid, it does not keep stress and transmit them to the neighboring regions.

Convergent rate of Indian plate after collision

The Himalayan mountain range occurred as a result of the Tertiary collision between the Indian and Asian plates (Fig. 4). The Collision, have developed in two stages (Le Pichon et al., 1992). The first stage involves convergence of the northward-drifting Indian subcontinent with a proto-Tibetan landmass during Late Cretaceous and Paleocene and the second stage involves formation of a fundamental crustal fracture within the Indian block during Late Eocene and Oligocene, and underthrusting of the Indian subcontinent along this fracture from Miocene to Recent.

Following breakup of the Gondwanaland, India commenced its northward movement at about 80 Ma ago. The convergence rate of Indian sub-plate under the Eurasian plate was cooperatively fast in the initial stage and that it has slowed over the last 50 Ma. Subsequent to collision, India continued to move north resulting in crustal thickening, deformation and high topographic elevation. Sea floor palaeomagnetic stripe data shows this movement to have been at about 15-20 cm/a (Trelor et al., 1992). The continued continental collision decreased to rate about 5 cm/a (Nakata et al., 1990; Upreti, 1999 and Johnson, 2002).

Patriat and Achache (1984) have showed three successive phases for account the Indo-Asia convergence rate. First, down to anomaly 23 (52 Ma) India was drifting northward with a mean velocity of 15-20 cm/a. Then, between anomaly 23 and anomaly 13 (36 Ma) the motion of India became rather erratic showing several changes in direction while the mean northward velocity was reduced to <10 cm/a. Finally, from anomaly 13 to the present, India resumed a stable northward direction of convergence with respect to Eurasia with a constant rate of <5 cm/a. The present convergence rate across the Himalayan range is 2 cm/a (Cattin and Avouac, 2000). Based on the above discussions, we

summarize the convergent rates during collisional period on Table 2, which are used for the present simulation.

Development history of Himalayan major structures after collision

Almost without exception, Geo-Scientists studying the Himalayan geologic evolution, generally assume that orogeny began in the Late Cretaceous-Early Eocene when India first collided with Asia (Yin et al., 1994; Le Fort, 1996). The Himalayan mountain system developed in a series of stages 30 to 50 million years ago (Figs. 5; Chemenda et al., 2000). Most models proposed for the evolution of Himalaya assume the zone of plate convergence shifted progressively and temporally towards the foreland during the mountain building process. An intracontinental thrust, the Main Central Thrust (MCT), is thought to be formed during the Miocene (Hodges et al., 1996). South of the MCT, Late Miocene movement slip occurred along the Main Boundary Thrust (MBT) (Meigs et al., 1995), and presently, the Main Frontal Thrust (MFT) is active (Yeats and Lillie, 1991). Convergence is primarily accommodated by the youngest structures, ones closest to the Indian foreland (Seeber and Gornitz, 1983). The most profound deformational event involving the interaction of lithospheric plates is collision between continents (Seeber et al., 1981). The Indian continent began to impinge on the Eurasian continent in the Eocene. The continuing northward compressional movement of India has produced intracontinental thrust (Le Fort, 1975; England and Molnar, 1993). The major structures are the MCT, MBT and MFT in Himalayas which are produced by the continual northward compressional movement of Indian sub-plate (Upreti, 1999). The initial continental subduction was characterized by low-compressional regime and therefore compression of Asia was weak. After the first break-off, 40-45 Ma ago the regime switched to a highly compressional mode and, therefore, the Asian plate was subjected to force full compression, but was probably still too strong to fail (Chemenda et al., 1995). Compression then gradually increased during tectonic underplating of the Indian lithosphere and at 30-35 Ma become sufficient to cause major failure within the Asian lithosphere, leading to the formation of major strike slip faults (Tapponnier et al., 1990). Starting from this stage, the Asian lithosphere became considerably weaker as a result the intense deformation and failure of different modes of this lithosphere is thus very likely (Chemenda et al., 1995). This stage terminates with initiation of first major thrust (MCT) 20-25 Ma. After this time, the underthrusting process continues along the MCT until the formations of second major thrust MBT at 10 Ma, and finally form the MFT at the present stage. Lyon-Caen and Molnar (1983) and Johnson (2002) also proposed that the MCT, MBT and MFT were created at 40, 20 and 10 Ma, whereas their formation was completed at 20, 10 and 0 Ma, respectively. From these sequences, it is clear that the formation of these major thrusts play the major role to mountain building process and to

shift the active subduction from north to south in the Himalayas. According to Lyon-Caen and Molnar (1983), DeCelles et al. (2001) and Johnson (2002), the subduction has been transferred from the Tsangbo suture at first 50 Ma to the thrust within the Tethyan sequence, then to the MCT (20-25 Ma), then to the MBT (10 Ma) and finally to the MFT (>0 Ma) in the Sub-Himalayan region.

Modeling

Elastic rheology

Finite element method is a numerical analysis for calculating the stress and strain in a complex geological structure of the earth. Stress and strain originate within the earth depending on the materials properties e.g. elastic, plastic and viscous. Here, we considered the elastic rheology under plane strain condition and proximity to failure value for deducing the stress and fault pattern in the Himalayas. Elasticity is the property of a material which causes it to be restored to its original shape after distortion. It is generally described in terms of the amount of deformation (strain) resulting from a given stress (Young's modulus). In isotropic continuum the elastic properties are independent in direction. The isotropic approximation is usually satisfactory for the earth's crust and mantle. On the basis of plate tectonic theory, the upper half of the lithosphere is referred to as elastic lithosphere (Turcotte and Schubert, 1982). The uppermost 20 and 30 km are the lithosphere of the continental crust and the oceanic crust as explained by Bott (1990) and Hassani et al. (1997), respectively. One of the fundamental postulates of plate tectonics is that the surface plates constituting the lithosphere don't deform significantly on a short geological time scale. The reason for considering the elastic behavior of lithosphere is to understand the stress state and their relevance to form the deform pattern in the study area.

A linear, isotropic, elastic solid is one in which stresses are linearly proportional to the strain and mechanical properties have no orientations. The behavior linear solids are more readily illustrated, if we consider the idealized situation where several of the stress and strain components vanish. These can then be applied to important geological problems.

Calculation of model

In performing the finite element analysis, initially a series of balanced geologic profiles (40 Ma-present) have been chosen from Lyon-Caen and Molnar (1983); Johnson (2002); Howladar and Hayashi (2004), where indicated the different development stages of Himalayan structures and tectonics. In order to produce a generalized geologic profiles, the geometry and topographic height of such profiles are reconstruct, modified and changed considering the previous thoughts on the tectonic development of Himalayas and present topographic map. All of the Himalayan geologists agree to state that the

Himalaya topographically was not so high till 20 Ma or later and it started to gain significant height from 10 Ma and finally the present stage, gaining the maximum height 8800 m. Still these tectonic processes are continuing due to the continual convergence of Indian sub-plate under the Eurasian plate. Considering this hypothesis, we primarily draw a generalized topographic profile for present stage in the central Himalaya using the topographic map of Nepal Himalayas from a topographic map. In this profile, we showed the maximum height in the Higher Himalaya (>8000m) from the sea level and other areas (Tethys, Lesser and Sub-Himalaya) are almost the same as with the present height. Consequently, we draw the 10, 20 and 40 Ma profiles (for details, see Fig. 7). After producing the primary profiles, we used successively a series of computer program associating with some other subprograms. All of the programs and subprograms used in this research have been developed by Hayashi (2002). The procedure of simulation follows a series of step for making models. The generalized flow chart of the simulation is shown in Fig. 6. Simplification and discretisation into triangular elements of the selected geological cross sections have been done manually. Then prepare a grid of entire nodal points of section with the Adobe Illustrator-10 as EPS file. Among these program, model trans.f, net.func, band.f, elas.f, stress.func, frame stress, frame failure etc. are the main programs. Moreover, some other subprograms also used for checking and trouble shoot. The common characteristic of every program is that they have a data file, one or more input file and out put files. Data file is required to make manually by inserting data for particular model. After that, filling the fill file with proper nomenclature of the output file. The out put file always used as the input file of each successive next program. In perusing the make model dat file the grid file run through several stages, i.e. X.get.func, XMag.f, XAd.f and input the element number in the accessories with nodal number at anti-clock wise and layer data in India.dat in accordance of layer in the model. After this stage the trans.f is run to produce input data file for net function and then net.f is applied to draw total triangular elements, nodal points and preferred value of X and Y axes. When all the data files (i.e. model.dat, India.dat, node.dat) and perfect net is produced, elas.dat file is prepared by inputting Poission's ratio density, Young's modulus value for each individual layer. Another accessory program band.f is applied to estimate the maximum value of the triangular element within the model before applying the elas.f file. The band.f program also controls the computing time, i.e. if the ibw value is large computing time will be long and small, it will be short. The elas.f is the program that generates the final data files which are used as input files to calculate the stress and illustrate the nature and distribution of stress in the model. The stress.f run with igor program to achieve the model with triangular elements, nodal points, magnitude of stress and orientation of the principal stress (σ_1) and intermediate principal stress (σ_3) in 2D condition. The two end members of the model are frame stress and failure element are calculated and illustrated by the frame stress.f and frame failure.f program, respectively.

Successively performing all of these stages mentioned above, make models, stress calculation and with the simulation results, it is easy to interpret and mimic the characteristics of stress field and their direct influence on deformation and development of faults or any other discontinuities in the converse tectonic events at the vicinity of the study area.

Numerical Simulation

Location of model

We produced a series of 2D finite element models (Fig. 7) considering the geologic profiles from central part of Nepal. The profile models A, B, C and D are rearranged and modified from Johnson (2002) which have shown by line A-A' in Fig. 2. The model profiles A, B, C and D are constructed to examine the idea that the MCT, MBT and MFT are created from the incipient zones assumed by Lyon- Caen and Molnar (1983) and Johnson (2002). The present profiles are simulated to show the present state of stress and faulting system with which can compare the presently observed stress and fault.

Geometry of models

The initial geometry of the numerical system (length, depth, structures and the dip of the model) is defined according to the cross profiles of central Nepal. The geologic profiles based mainly the seismic reflection profiles, which show the north to south verging thrusts. The length and depth of models A, B, C and D are 235x35, 210x45, 225x40, 150x30 km, respectively (Fig. 7). The total area of all models is divided into a number of triangular elements with three nodes. The total number of elements and node points area of all models varies from one another are shown in Fig. 10.

The grid of all models have been designed and modified to permit assignments of different rigidities for numerous tectonic units. Each model represented six or seven major structural units as their regional tectonic setting and they are divided as follows: Base of Tibetan oceanic crust, Base of Indian continental crust, Tethys Himalaya, Higher Himalaya, Lesser Himalaya and Sub-Himalaya as shown in Table 3. The major faults in models are ITS, STDS, MCT, MBT, MFT and MHT.

Physical constants of layer

We simplified of all models and divided them into different layers and choose most and major common rocks for each layer to skip the complexity of calculations for each model. The rocks of each layer are characterized by the physical parameters such as Young's modulus, Poisson's ratio, density, cohesion and internal friction angle. Within the general simplifications of all models, the choice of these parameters of rocks offer a good approximation. The elastic constants include the Young's modulus (E), Poisson's ratio (ν). The actual values of these parameters are not well constrained. As a consequence, we tested all models with a variety of values in order to explore the effects of changes in

parameters and their sensitivity to results. Five parameters (Young's modulus, Poisson's ratio, density, cohesion and angle of internal friction) for each layer are shown in Tables 3. Because several major structural units have quite different rheological properties. The abundance of these parameters of rock in each layer is shown in Table 4 and Fig. 8 and the comparison of each model layer parameters is shown in Fig. 9. The highest value of all mechanical properties is taken for Tibetan oceanic crust then Indian continental crust, Higher Himalaya, Lesser Himalaya, Tethys Himalaya, and the lowest for Sub-Himalaya.

The Himalayan profiles which we used, consist of six or seven rock layers shown in Fig. 7. Tibetan oceanic crust and Indian continental crust are considered to be composed of basalt and sandstone, gneiss and granite. The Higher Himalaya is composed of gneiss and schist which form the basement of the Tethys Himalaya with various kinds of leucogranite from Eocene to Middle Miocene and later (Searly *el al.*, 1987). The age of Tethys Himalaya ranges from Cambrian to Tertiary period. Lesser Himalaya comprises relatively high-grade phyllite whose age is still controversial (Kaneko, 1997; Upreti, 1999). The Sub-Himalaya comprises of Neogene to Quaternary and recent fluvial sedimentary rocks (Kano, 1984; Upreti, 1999). The incipient zones of MCT, MBT and MFT are considered to be covered by the metasedimentary and clastic sedimentary rocks, respectively.

We consider with regards to the rock layer properties that there is a tendency shown in Figs. 8 and 9. The older model profile might be composed of more harder rocks with respect to the younger profile and the older the rock layer is, the larger the rock properties (density, Young's modulus and cohesion) are, while the lesser the friction angle is; and Poisson's ratio is considered constant for all models shown in Table 4.

Boundary condition

Boundary condition is important for evaluating the stress field and fault pattern. The magnitudes of stress are directly related to the elastic properties of rocks and the imposed displacement boundary conditions. In order to mimics natural situation, we imposed displacement boundary conditions instead of forces because the velocity of plate movement between the Indian sub-plate and Eurasian plate is known. The boundary conditions are same for four models except for the value of displacement. The different convergent displacements, which derived from the different convergent velocities multiplied by period, are imposed perpendicular to the right-side wall BC as already mentioned in Table 2 and Fig. 10. The left side edge AD is fixed horizontally. Node A is fixed. As the value of displacement is given proportional to the distance from the point A along bottom line AB, the imposed displacements shown by arrows in Fig. 10. These imposed displacements are vectors which have both components of horizontal and vertical. The upper boundary CD is free so as the earth's surface.

Faulting area identification by proximity to failure (P_f) under Mohr coulomb criterion

The Mohr-Coulomb failure criterion has been widely used for geotechnical as well as

geological applications. It assumes that failure is controlled by the maximum shear stress and that this failure shear stress depends on the normal stress. In the present simulation, we primarily computed the stress and then the failure elements as a function of rock layer properties and displacement boundary condition under plane strain state model. The generalized plane strain theory used in assumes that the model lies between two bounding planes, which may move as rigid bodies with respect to each other. In the plane strain condition, the deformation of the model is independent of position with respect to the thickness direction, so the relative motion of the two planes causes a direct strain of the thickness direction only. In order to identify the deformed area (faulting area) of the present plane strain model, we used the proximity to failure (P_f; Melosh and Williams, 1989) under Mohr Coulomb criterion. More interestingly, proximity to failure parameter may help to identify which parts of the model are far away from the yielding stress and thus can be considered to be stable and strong. In general the proximity to failure is defined as the ratio between the effective stress and the failure stress (yield stress). Where this ratio is one or more than one, the effective stress has reached the yield stress limit and rock failure occurs. In the numerical calculation, all of the deformations are directly related with the failure of rocks thus we considered these failures as fault in the simulated models.

Classification of faults under Anderson theory (1951)

The failure elements (fault) are calculated based on the P_f value under Mohr Coulomb criterion. While the main aim of the study is to develop the fault in the Himalayan region, thus it is necessary to classify the computed faults. Consequently, faults are classified appealing the Anderson theory (1951). He assumed that all the principal stresses are either horizontal or vertical. This theory predicts three types of observed faults, thrust, strike-slip and normal fault, depending on which the nature of distribution of principal stresses. Andersonian predictions of the orientation of each type of fault are consistent with many observations (e.g. Sibson, 1994).

Significance of numerical modeling

The model focuses on aspect of the Himalayan region where the crustal deformation is dominated by brittle processes, which are approximated by an elastic rheology. The elastic limit obviously varies with depth, so that the values adopted represent an average strength base on the grade of rocks for the model. The depth of brittle deformation is about 20-30 km. Most surface earthquake hypocenters concentrate in the depth range 5-20 km that is the upper half of the continental crust (Lyon-Caen and Molnar, 1983). Bott (1990) pointed out that the uppermost 20 km of the continental crust is elastic, representing the strong and cool layer of the upper lithosphere. However, in the collision zone, where the cold lithosphere is underthrust and elastic behavior occurs at greater depths. The aim of the present modeling is discussing the stress and fault in the brittle layer of the upper crust through a simple 2D analysis. The results of simulation are

certainly well compared and co-related with the previous studies. The main limitation of the model is that it is strictly a 2D elastic model. In fact, to elucidate the more realistic deformation pattern in a mountain belt, a 3D elasto-plastic model is required

Results

Characteristics of computed stress field

The stress fields of all models are simulated primarily based on the seismic reflection profiles with elastic rheology. As the distribution of stress in every model, which are presented by principal stresses (σ_1 and σ_3) in the triangular domain. The values of principal stresses are negative in everywhere, that is, the stresses are compressive. For the general sense of absolute value, the greater one was named as the maximum principal stress (σ_1) and the other is the minimum principal stress (σ_3). In every figures (Fig. 11), each pair of lines which is perpendicular each other and whose lengths indicate the absolute values, one represents the maximum principal stress (σ_1) and the other is the minimum principal stress (σ_3) of the respective triangle. Stresses of all models are almost similar to each other, though their convergent displacement boundary conditions are different. The stress pattern shows the compressive nature of principal stresses in all part of the models (Fig. 11). No tensional stress observed in the models. The magnitude and orientation of the principal stresses primarily depend on boundary condition and rock layer properties. It is always difficult to decide the value of rock properties. Thus, we examine a lot of experiments changing the values of rock layers property on the results. The values are finally fixed and listed in Table 4. The displacement imposed as boundary condition hardly affects the tendency of stress distribution. The direction of maximum principal stress is almost the same for models A, B, C and D whereas σ_1 deviated slightly from the horizontal along the bottom part of the Tibetan oceanic crust, Higher Himalaya, Lesser Himalaya and the base of Indian continental crust. Magnitudes of compressive stresses σ_1 and σ_3 are increased gradually with depth to reach the highest limit along the basal part of all models (Figs. 11 and 12). In case of the upper part of models, the magnitudes of principal stresses are very low and somewhere near to zero (Fig. 12)

Distribution differential stress and maximum shearing stress

The differential stress is the difference of maximum principal stresses values σ_1 and σ_2, and maximum shearing stress is the maximum shearing stress values of σ_1 and σ_2 that deform a body. These stresses parameters are denoted by D_S and τ_{max}, respectively. In the numerical modeling, these D_S and τ_{max} values are used as a primary clue to identify the areas of the models where the deformations may be. We thus being estimating the D_S and τ_{max} to investigate the stress field associated with deformation tendencies of four models A, B, C and D. The estimated values of these stresses are shown in Fig. 13,

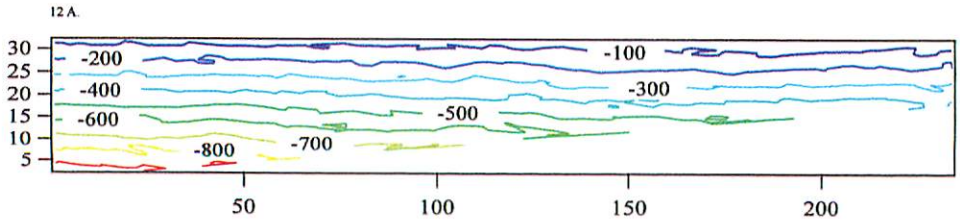

Fig.12 A. Contour map of σ_1 (MPa) in model A.

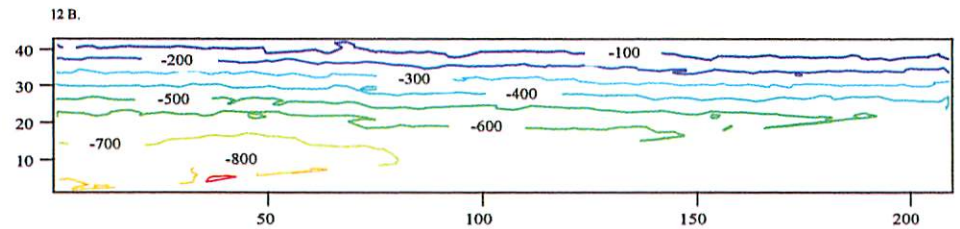

Fig.12 B. Contour map of σ_1 (MPa) in model B.

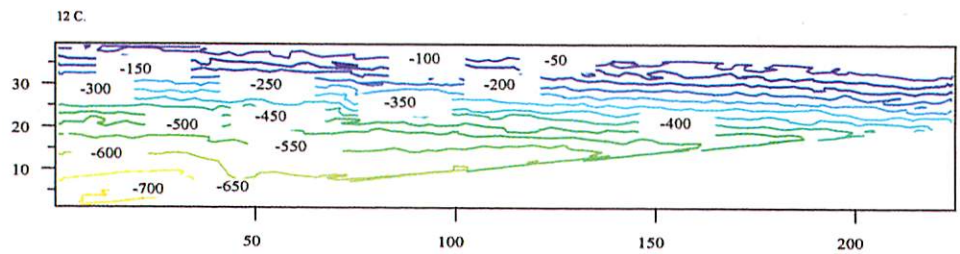

Fig.12 C. Contour map of σ_1 (MPa) in model C.

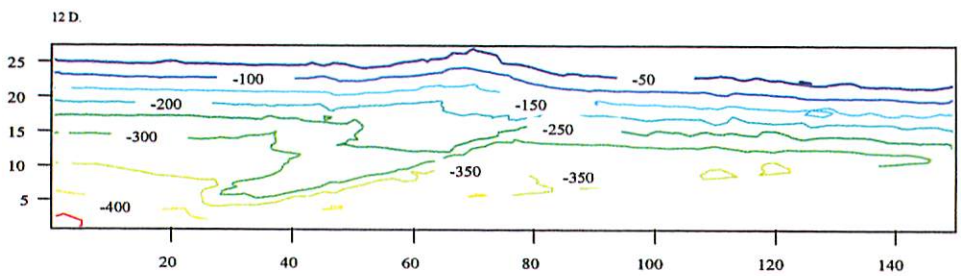

Fig.12 D. Contour map of σ_1 (MPa) in model D.

respectively. The maximum values of these stresses are commonly observed in shallow depth and in the incipient zones of MCT, MBT and MFT whereas the intermediate and minimum values are varied in the middle and deeper part of the models, respectively. The some of the representative values of D_S and τ_{max} of model A, B, C and D are shown in Table 5. Thus, from the distribution of these stresses in the models, it can be stated that

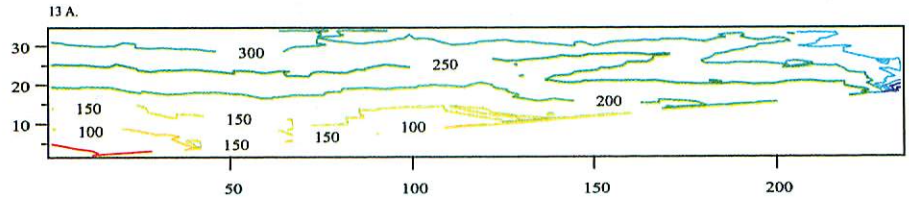

Fig.13 A. Contour map of τ_{max} (MPa) in model A.

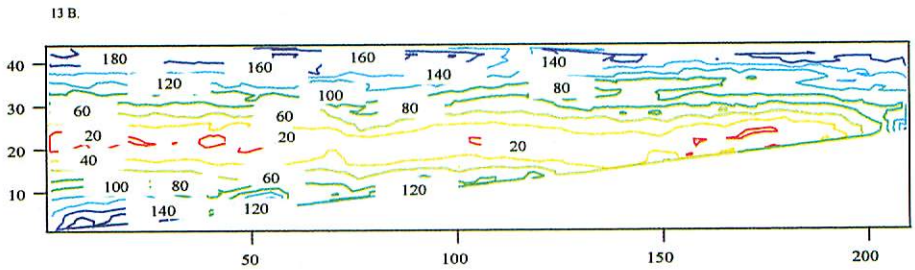

Fig.13 B. Contour map of τ_{max} (MPa) in model B.

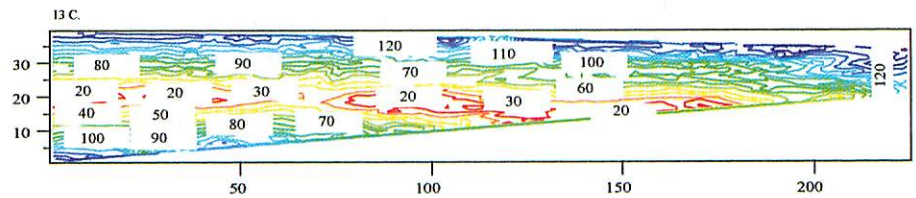

Fig.13 C. Contour map of τ_{max} (MPa) in model C.

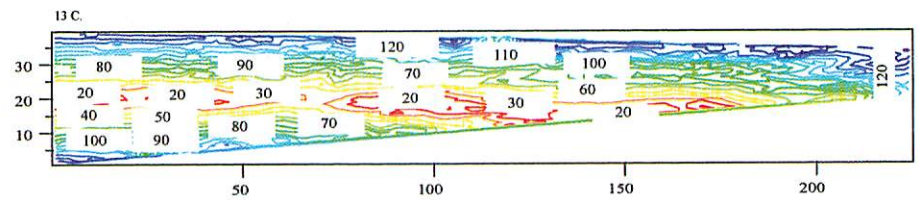

Fig.13 D. Contour map of τ_{max} (MPa) in model D.

the deformations might take place in the shallow depth and incipient zones of the major thrusts than the deeper area.

Simulated failure pattern

To estimate the role of displacement on forming the failure element under plane strain condition, we calculate the proximity to failure (P_f) which is proposed by Melosh and Williams (1989), from the principal stresses σ_1 and σ_3. The method how to calculate P_f is described by Howladar and Hayashi (2003). we determined the failure element

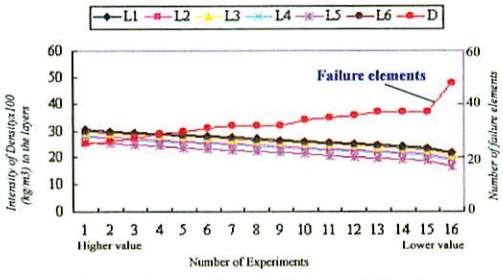

A1. Intensity of density to rthe layers and their influence to the failure elements.

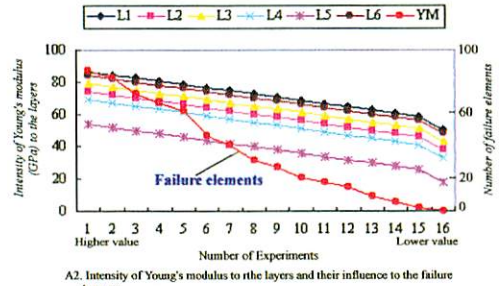

A2. Intensity of Young's modulus to rthe layers and their influence to the failure elements.

Fig. 14. continue.....

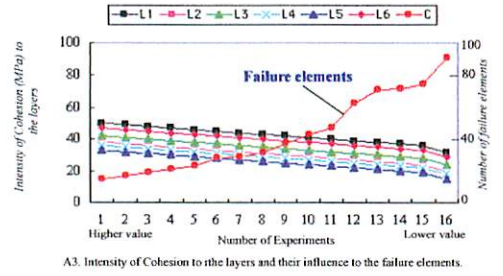

A3. Intensity of Cohesion to rthe layers and their influence to the failure elements.

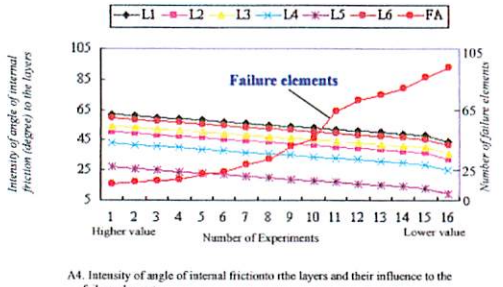

A4. Intensity of angle of internal frictionto rthe layers and their influence to the failure elements.

Fig.14. The values of each layer parameters (D=density, YM=Young's modulus, C=cohesion and FA=angle of internal friction) and their influence to the failure Elements (faults) in the representative model A. Here, L 1= Tibetan oceanic crust, L 2=Tethys Himalay, L 3=Higher Himalaya, L4=Lesser Himalaya, L5=Sub-Himalaya, L 6= Base of Indian Continental crust. (note: Individual influence of Poisson's ratio does not included here while it has been considered as a constant parameters for all cases).

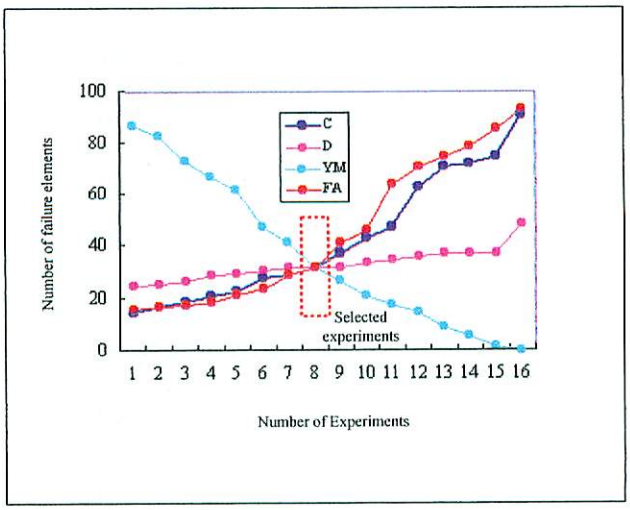

Fig.15. Influence of layer parameters to the failure elements (faults). Here, D=density, YM=Young's modulus, C=cohesion and FA=angle of internal Friction.

considering the proximity to failure (P_f) under the Mohr Coulomb failure criterion. If the value of P_f is equal or larger than 1.0, failure occurs.

Simulation shows that failure elements take mostly place within the Tibetan oceanic crust, Tethys Himalaya, Higher Himalaya, incipient zone of major thrusts, Lesser Himalaya and Sub-Himalaya from Late Eocene to present (Fig. 16). The compressive stress oriented horizontally in shallower depth of the Tethys Himalaya, incipient zone of MCT, MBT and MFT, Lesser Himalaya and Sub-Himalaya. This orientation of the principal stress axis decides the direction of thrust faults, while the stress difference σ_1-σ_3 generates these faults, which are highly concentrated within the incipient zones than other rock layers for models A, B, C and D. The thrust faults predicted in the models which are initiate at depth primarily and then transmit to shallower region with increasing convergent displacement and finally they tend to propagate southward. Faulting tendency in the models change towards shallow depth and south. In the north, where detachment is deep, and rock strength is great, showing very few failure elements (faults). In the south, where detachment is shallower, and the rock strength is weaker, foreland strata are highly deformed by faulting above shallower dipping detachment which mimic the structures in the frontal part of Himalayas, where imbricate thrusting is common. These results also suggest that the comparatively younger rock formations are more frequent to form the fault where the magnitudes of principal stresses are very low.

Influence of convergence displacement

The mode of stress and fault is primarily influenced by model boundary conditions (amount of imposed convergent displacement). With regards to the boundary condition, we performed a number of experiments with different combinations of convergence

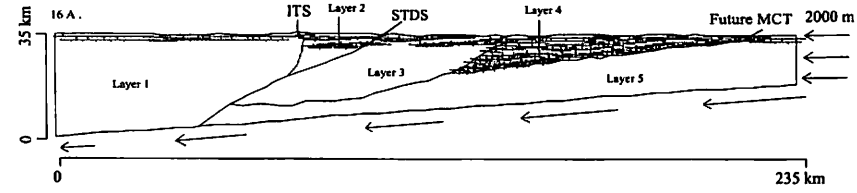

Fig.16 A. Distribution of principal stress of failure elements under 2000 m convergence displacement in model A. Layer 1= Tibetan oceanic crust, Layer 2= Tethys Himalaya, layer 3= Higher Himalaya, layer, 4= Incipient zone of MCT and layer 5=Base of Indian continental crust.

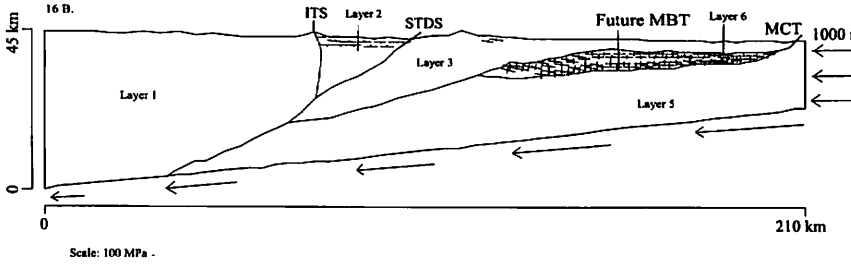

Fig.16 B. Distribution of principal stress of failure elements under 1000 m convergence displacement in model B. Layer 1, 2, 3 and 5 are same as previous figure and here the layer 6= Incipient zone of MBT.

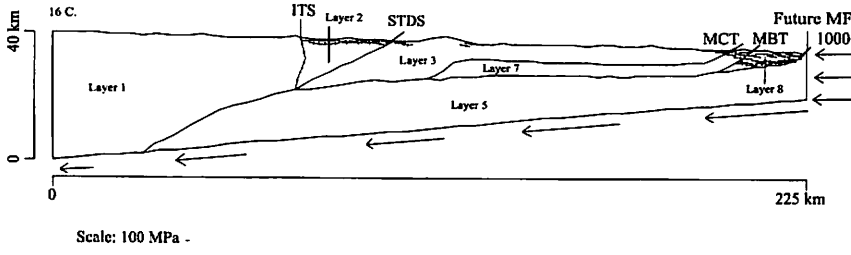

Fig.16 C. Distribution of principal stress of failure elements under 1000 m convergence displacement in model C. Layer 1, 2, 3 and 5 are same as previous figure. Here the layer 7 and 8= Lesser Himalaya and Incipient zone of MFT, respectively.

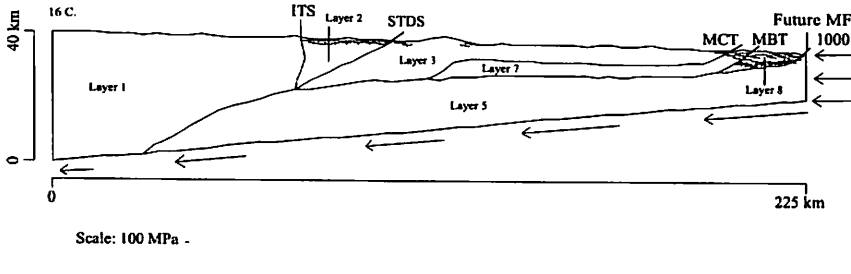

Fig.16 D. Distribution of principal stress of failure elements under 400 m convergence displacement in model D. Layer 1, 2, 3, 5 and 7 are same as previous figure and here the layer 9= Sub-Himalaya.

Tectonic divisions	corresponding layer nos.	Rock types	Metamorphic zone	Intensity of faulting
- - - MFT - - - Sub-Himalaya (SH)	9	Sandstone and siltstone	unmetamorphosed	large number of fault developed
- - - MBT - - - Lesser Himalaya (LH)	7	Phyllite, limestone and sandstone	biotite-chlorite	fault developed
- - - MCT - - - Higher Himalaya (HH)	3	Gneiss and granite	kyanite	few fault developed
- - - STDS - - - Tethys Himalaya (TH)	2	Limestone and sandstone	chlorite-biotite-garnet	fault developed
- - - ITS - - - Tibetan oceanic crust (TOC)	1	Basalt	no data are avialable	fault developed only in the 40 Ma model
Indian Continental Crust (ICC)	5	Gneiss, granite and schist	metamorphosed	no fault developed
Incipient zones of MCT, MBT and MFT	4, 6 and 8	Metasediments and clastic sediments	no data are avialable	large number of fault developed

Fig.17. Faulting vulnerability of different rock units of Himalayas.

displacement boundary conditions along the South-West to North-East direction. The amount of displacement boundary conditions have proportionally distributed to the horizontal length (x-axis) of all models that have shown by the length of line with arrow in Fig. 10. The distribution of stress has approximately similar in all models and no drastic change has observed during the experiments. The total period of simulation, it is observed that the stress and faults of all models are similar to each other, whereas with increasing convergence displacement, the magnitude of principal stresses and failure elements increase slightly which is clearly observed in the Tethys, Lesser Himalay and Sub-Himalayan rock units (Figs. 11 and 16). Thus primarily, the magnitude of stresses and faults are governed by the model boundary conditions.

Influence of layer rheology

In order to evaluate the influence of layer rheology, initially we divided of all models into different layers as shown in Fig. 7 with different rock properties. We choose the most dominant rocks for each layer to find out their influence to the stress field and fault. The distribution of major rocks of such layers are gneiss, granite, metasediments, phyllite, limestone, siltstone and sandstone listed in Table 3. The physical properties of these rocks are defined by five parameters such as Young's modulus, Poisson's ratio, density, cohesion and angle of internal friction. With respect to influence of layers rock properties, it is attempted to investigate the mode of stress and fault for different layer properties in order to identify the suitable condition that are likely to led to form the fault in the model. For this purpose, layer parameters of the model are varied in several times and their influences are shown in Fig. 14. Finally the most reasonable parameters of the

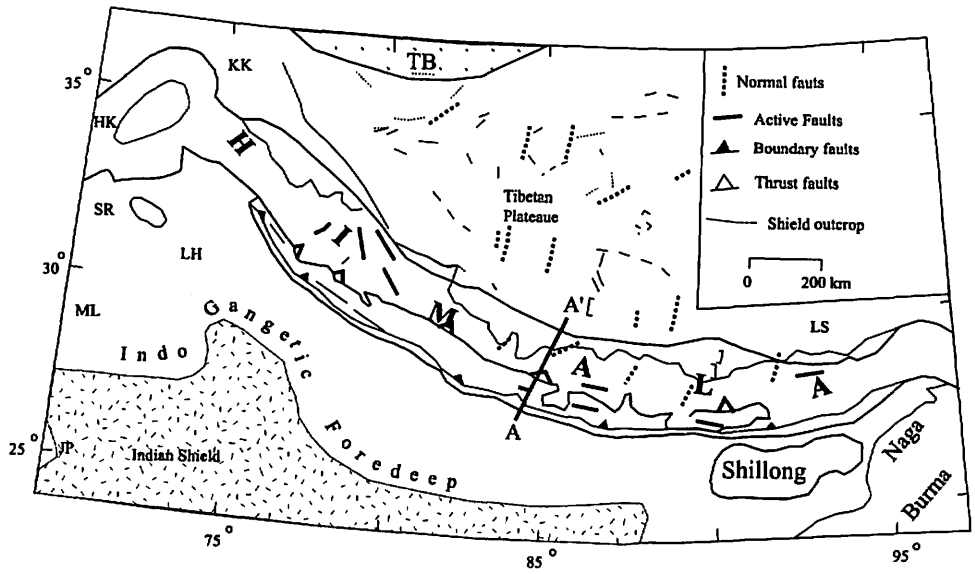

Fig.18. Distribution of active faults around central Himalayan range after Molnar and Tapponnier (1978) and Seebar et al. (1981). A-A' line shows the location of model profiles. TB= Tarim Basin, SR=Salt Range, LH=Lahore, ML=Multan, HK=Hindu Kush, KK=Karakoram, JP=Jodhpur, LS=Lhasa.

layers have been determined which show the very similar stress and fault pattern with field data in Himalayas are shown in Table 4. Generally, It is observed that the Young's modulus, cohesion and angle of internal friction are significantly effective to increase the number of failure elements in the Tethys Himalaya, Lesser Himalaya and Sub-Himalaya than other properties. Unfortunately, layer properties have no significant effect on stress magnitude and orientation in models. Thus the magnitude of stresses and faults are not only governed by the model boundary conditions alone but also by the applied values of different layer's rheology of the models.

Discussions

How to set-up models

The finite element models presented and discussed above have been produced from a series of balanced geologic profiles after Johnson (2002). In order to produce a generalized geologic profiles, the geometry and topographic height of such profiles are reconstruct, modified and changed considering the previous thoughts on the tectonic development of Himalayas by Molnar and Tapponnier, 1975; Lyon-Caen and Molnar, 1983; Chemenda et al., 1995; Kaneko, 1997; Yin and Harrison, 2000; Chemenda et al., 2000; Johnson, 2002 and so on and present topographic map. All of the Himalayan geologists agree to state that the Himalayas topographically was not so high till 20 Ma or later and

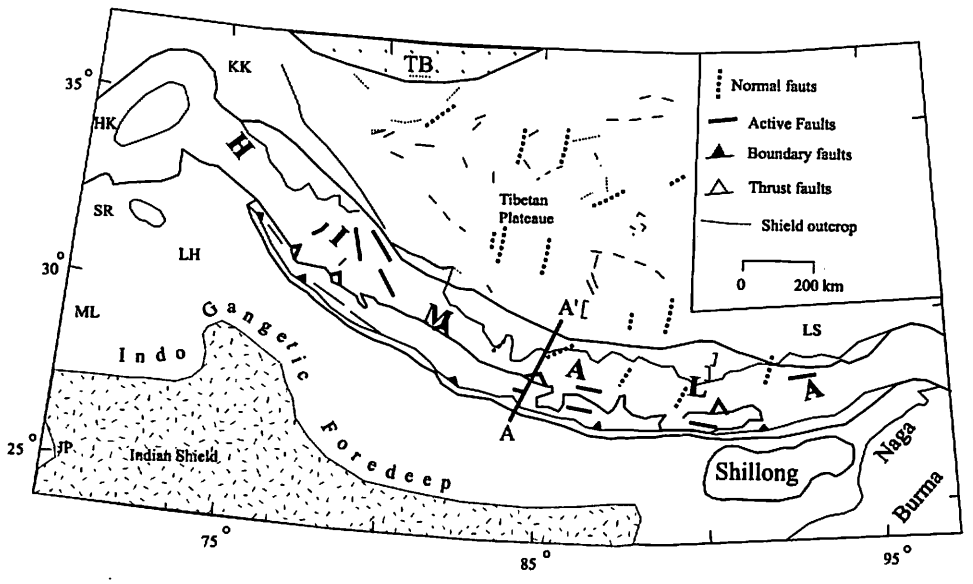

Fig.19. Faulting pattern from the focal mechanism solutions of earthquakes in the Himalayas and surrounding regions modified after Chandra (1978).

it started to gain significant height from 10 Ma and finally the present stage, gaining the maximum height ~8800 m. Still these tectonic processes are continuing due to the continual convergence of Indian sub-plate under the Eurasian plate. Considering this hypothesis, we primarily draw a generalized topographic profile for present stage in the central Nepal using the topographic map of Nepal Himalayas from a topographic map. In this profile, we showed the maximum height in the Higher Himalaya (>8000m) from sea level and other areas (Tethys, Lesser and Sub-Himalaya) are almost the same as with the present height. Consequently, we draw the 10, 20 and 40 Ma profiles (for details, see Fig. 7). After producing the primary profiles, finite element method have been applied with 2D space and simple geometry of the convergent belt, assuming the homogeneous and isotropic material within the individual layers. In nature the behavior of rocks are not homogeneous and isotropic. Furthermore, the rocks layer properties are used in these simulations are not experimentally determined as a consequence, we have tested all the models with varying values in order to find its the effect on the stress field and failure elements. Finally we adopted only the most suitable set of layer properties for the calculation which are shown in Table 4. We assumed that the crust behaves as elastically though it is visco-elastic-plastic in nature. Although the present simulated models remain simple and assumed data are consistent with known field data.

How to decide convergent displacement

The displacement boundary condition simply corresponds to the convergence of the Eurasian plate relative to the Indian subplate. According to Patriat and Achache (1984),

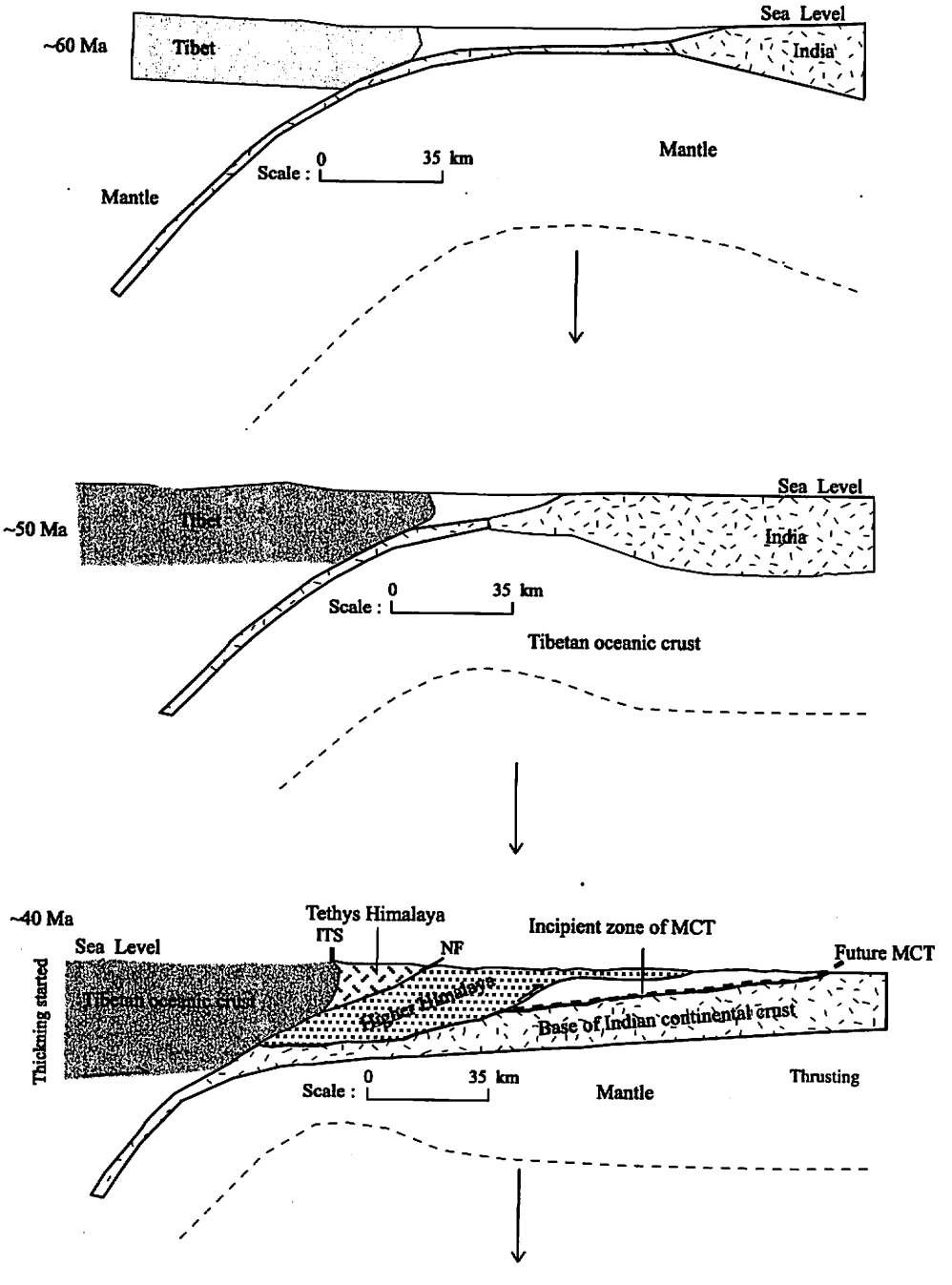

Fig.20. Schematic representation of the development stage of geo-tectonic features (mainly MCT, MBT and MFT) of Himalaya based on the incipient zone of MCT, MBT and MFT with the sequential decreasing of convergence rate of Indian plate beneath the Eurasian plate. This is created after Chemenda et al. (2000) and Johnson, (2002).

Continuation of Fig. 20

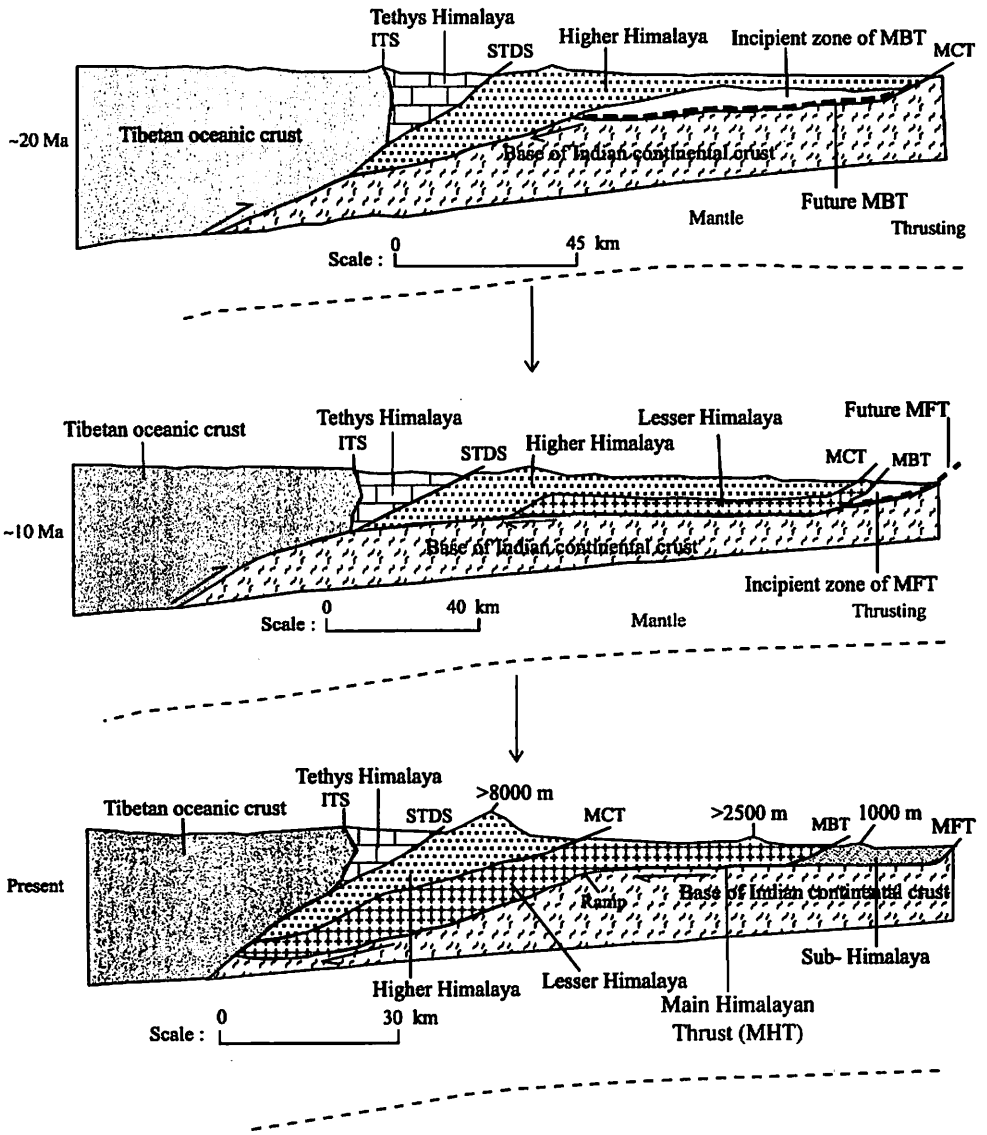

the Indo-Asia convergence rate first, down to anomaly 23 (52 Ma) when India was drifting northward with a mean velocity of 15-20 cm/a. Then, between anomaly 23 and anomaly 13 (36 Ma) the motion of India became rather erratic showing several changes in direction while the mean northward velocity was reduced to <10 cm/a. Finally, from anomaly 13 to the present, India resumed a stable northward direction of convergence with respect to Eurasia with a constant rate of <5 cm/a.

The Indian plate moves north-northeast at a rate of 44-61 mm/a relative to Eurasia/Siberia (Armijo et al., 1986; Bilham et al., 1997). GPS geodesy has established the

rate of India-Asia convergence at 54 ± 4 mm/a. Only about 30 percent (e.g. 18 ± 2 mm/a) of the India-Asia convergence is absorbed across the Himalaya; thus, the average rate of accommodation derived on the basis of slip rates of great earthquakes is ~17 mm/a. Recent GPS measurements along the Delhi-Malari and Delhi-Milam sections across the Kumaun Himalaya show that the Tethyan domain beyond the Higher Himalaya is advancing southward at the rate of 18 to 20 mm/a. Sea floor palaeomagnetic stripe data shows this movement to have been at about 15-20 cm/a (Trelor et al., 1992). The continued continental collision decreased to rate about 5 cm/a (Nakata et al., 1990, Upreti, 1999 and Johnson, 2002). The present convergence rate across the Himalayan range is 2 cm/a (Cattin and Avouac, 2000). On the basis of these histories of convergence rates between India and Eurasia after collision, we choose 2000 m (10 cm/a) for model A, 1000 m (5 cm/a) for Model B and C and 400 m (2 cm/a) for present model as the displacement boundary conditions.

Justification of elasticity of earth crust

The finite element models are assumed in elastic state with failure criterion in the numerical experiment. The elastic assumption is based on the plate tectonic theory (Turcotte and Schubert, 1982). The continental lithosphere is considered to be internally rigid. The rigidity of the lithosphere allows the plate to transmit elastic stress during geological time intervals. Generally the continental lithosphere has thickness of more than 100 km, though the thickness of the models is less than 60 km. Although the entire lithosphere is not effective in transmitting elastic stress, the upper half of it is sufficiently rigid. This fraction of the lithosphere is referred to as the elastic lithosphere. Bott (1990) pointed that the uppermost 20 km of the continental crust is elastic, representing the strong and cool layer of upper lithosphere. Hassani et al. (1997) fixed the elastic thickness to be >30 km for the oceanic lithosphere. Thus the elastic modeling method is acceptable for the finite element models used. Gerbault et al. (1998) discussed in detail about the prediction of deformation pattern faulting from the theory of elasticity. In their view, elastic approach is relatively simple, intuitive and preferable to predict faulting in nature, because it is consistent with many field observations of the fault orientation at small as well as regional scale (e.g. Sibson, 1994). In the present numerical analysis, the rheology has been justified experimentally. In order to do it, primarily we performed lots of test calculations for each layers of four models. In the second stage, we choose 16 reasonable test calculations for selecting the final parameters and their empirical values. From these experiments, it is clear that the number of failure elements increase rapidly for Young's modulus case and decrease for density, cohesion and angle of internal friction angle cases when the most highest empirical values are considered for each layers parameters of the test experiments besides they reflects reverse tendency for the most lowest values experiments, respectively are shown in Fig. 15. Interestingly, the experiment 8 reflects the equilibrium state for all elastic parameters in the models. Thus, we selected this

experiment for the present simulation which also directly consistent and well matched with known field data.

General distribution of stress in Himalayas

Himalayas and neighboring areas are the indicators of recent and sub-recent crustal movements due to the continental collision between the Indian and Eurasian plates. The relative motions between these plates influence the regional stress field and structures in the region. In recent years, the characteristics of regional stress has been interpreted by many authors (Molnar et al., 1977; Chandra 1978; Cloetingh and Wortel, 1986; Shanker et al., 2002; Howladar and Hayashi, 2003 & 2004 and so on. The direction of maximum horizontal shortening or horizontal compressive stress along the eastern Himalayan front approximately N-S, parallel to the relative motions o the two plates (Nakata et al., 1990). However along the southern margin of the Eurasian plate, they are NE-SW in the western Himalayan front and NW-SE to E-W in the Kirthern-Sulaiman front which is not consistent with the relative motions. He further noted that the direction of has changed following the change in direction of the relative motion between the Indian sub-plate and the tectonic sliver, which have detached together along the transcurrent faults in the Eurasian plates. These studies clearly indicate that the regional direction of maximum principal stress axis is consistent with the relative plate motions at least in the central part of Himalayan region. The stress state in the northern most part of Himalaya is quite different due to its different tectonic regime and structural configurations. Immediately north of the highest peak of the Himalayas, the tectonic regime is dominated by east-west extension, which is dominantly characterized by the strike-slip and normal fault system (Blisniuk et al., 2001). The reasons of the extension in this region and its relationship to the change in elevation of Tibetan plateau are of the fundamental importance to the continental collision. The fault plane solutions of Himalayas (Molnar et al., 1977; Chandra, 1978) indicate that the large component of thrust fault (dominantly) and normal and strike fault under compressive and extensional stress regime.

Although the regional stress in the colliding boundary generally considered to be dominated by the convergence of the Indian and Eurasian plates, the direction of the compressive stress axis is not consistent everywhere regionally in the region. The direction of compressive stress deduced from focal mechanism solution is at right angle to the topographical trend on all sides of the Indian Peninsula (Verma, 1997). However it is noteworthy that the compressive stress field dominant over the whole Himalayan region due to the continuous NS compressional influences of Indian plate. Simulated models also show the compressive stress in all stages of computation (Fig. 11), which are a good agreement with the local as well as regional compressive stresses field in the Himalayas.

Faulting vulnerability of different grade rock layers

These relationships have been drawn based on the distribution of simulated faults in the high-low grade rocks layer of the models. The model profiles have taken from the

central Nepal Himalayan region underlain by various kinds of metamorphic-sedimentary rocks, including psammitic schist, augen gneiss, metapelites, quartzite, metabesites, migmatite, orthogneis, phyllite, sandstone, siltstone, limestone and so on (Hashimoto et al., 1973; Le Fort, 1975; Arita, 1983; Sakai, 1985; Hubbard, 1996; Upreti, 1999). The rocks of the area are divided into several metamorphic groups based on the changes of mineral assemblages (Fig. 17; Kaneko, 1995 & 1997). From the viewpoint of rock grade, the Lesser Himalayan Sequence and Tethys Himalayan Sequences are belong to the chlorite, biotite and garnet zones whereas the kyanite zone mainly dominated in the Higher Himalayan Sequence. The Sub-Himalaya comprises of recent sedimentary rocks (Tables 3 and 4; Upreti, 1999). Such kinds of rocks are adopted to examine fault in the proposed models. It is observed that the simulated thrust faults are frequently developed within the low-grade rock units such as Tethys Himalaya, Lesser Himalaya and Sub-Himalaya (Fig. 16). Thus it is obvious that the low-grade rock layers might be more vulnerable to develop the faults than in the high-grade rock layers of the regime.

Relations between simulated faults and behavior of major tectonic Structures

The major tectonic structures of the Himalayas are MHT, STDS, MCT, MBT and MFT which are separated the different geologic units such as Tethys Himalaya, Higher Himalaya, Lesser Himalaya, Sub-Himalauya and basement of Indian continental crust. In models, MFT separates the Sub-Himalaya and Indian Gangetic plain, MBT divided the Higher Himalaya and Lesser Himalaya, MHT shows it's position about 5-7 km below Sub-Himalaya in the south and increase gradually it's depth and steepness towards north. STDS marks the boundary between the Higher Himalaya and Tethys Himalaya. The behavior of major tectonic structures in Himalayas is quite different from one another. However, the active faults in the Himalayas are MCT and MBT (Joshi and Patel, 1997) and MFT (Lyon-Caen and Molnar, 1983; Lave and Avouac, 2000). MCT is thought to be active during Miocene (Hodges *et al.*, 1996). Slip movement in south of the MCT occurred along the MBT (Meigs *et al.*, 1995) in Late Miocene. MFT is now active (Yeats *et al.*, 1991; Upreti, 1999). Despite these active intercontinental thrusts, there are also many local active faults are shown by active fault studies (Fig. 18; Molnar and Tapponnier, 1978; Seeber et al., 1981 and Nakata, 1989). These active fault or thrusts are also the direct indicator of the crustal movements due to the collision between the Indian and Eurasian plate (Molnar and Tapponnier, 1975; Lyon-Caen and Molnar, 1983; Nakata *et al.*, 1984). We believe that these active faults or thrusts have greatly influenced stress field and structures since the early Eocene in the region. In the present analysis, we deduced the stress distribution and faults by adopting finite element method which shows the close similarities with active structures in the Himalayas. The general features of the stress field and fault development are shown in Figs. 11-16. The stress fields show nearly the same characteristics for four models A, B, C and D (Fig. 11). Within all layers, the compressive σ_1 tends to be nearly horizontal, and increases its area from deeper to

shallower area.

The present simulation shows that thrust faults are formed parallel along the real MBT, MFT and the real STDS in shallow depth as illustrated in Fig. 16. The MBT and MFT is the major thrusts in Himalayas which were produced within the compressional wedge during the Cenozoic period (Searly *et al.*, 1987; Mugnier et al., 1992; Thakur *et al.*, 2000). The present simulation shows the compressive σ_1 is directed horizontally throughout the elongation of such thrusts as shown in Fig. 16. We believe that the failed zones caused by the horizontal σ_1 and formed the thrust faults in all stages of models. Searle (1986); Searly *et al.* (1987); Nakata (1989, 1990) states that the south directed thrust faults are observed in shallow depth along the MBT and MFT from their the early development time to present state, which support the existence of simulated thrust faults in the models.

Comparison with the previous studies

Simulated compressive stress fields (Fig. 11) coincide with continuous NS compressional influences of Indian plate to the Himalayan profiles. The calculated compressive stress fields also good agreement with the local as well as regional compressive stresses in the Himalayas (Molnar et al., 1977; Chandra 1978; Nakata et al. 1990; Shanker et al. 2002; Howladar and Hayashi, 2003 & 2004). The failure elements predicted by the simulation in models are recognized within the Tethys Himalaya, Higher Himalaya, incipient zones and Lesser Himalaya, where compressive stress oriented horizontally which leads to the formation of the thrust faults in the proposed models (Fig. 16). Searle (1983a, 1986) and Searly *et al.* (1987) reported that the progressive south directed thrust fault development after the collision during middle Tertiary period along central part of Himalaya which is the explanation of simulated thrust fault for model A, B and C. After Eocene, thrust deformation spreads southward. Consequently, thrust faults are observed in the Tethys Himalaya, then Higher Himalaya, Lesser Himalaya and finally in the Sub-Himalaya at present stage (Fig. 16). These simulated faults of present stage profiles are well corresponded with the field fault data of Himalayas are shown in Fig. 17 (Molnar and Tappornnier, 1978; Seebar et al., 1981; Nakata, 1984, 1989; Thakur et al., 2000; Thakur, 2004; Chamlagain and Hayashi, 2004).

The numerical models predicted the thrust faults in the present stage are also consistent with the focal mechanism solutions of earthquakes in the region (Molnar et al., 1977; Chandra, 1978). Focal mechanism solutions of earthquakes gave the same general pattern of thrust faulting in the Himalayan region (Fig. 19). These present stage thrust faults seem to be associated with the major intra-continental thrust MCT, MBT and MFT (Nakata, 1989). The existence of such fault in the frontal part of the Himalayas is in agreement with neotectonic movements along the MFT in the Nepal Himalaya (Nakata *et al.*, 1984). It is observed that thrust fault is intensely localized to southward from Tethys Himalaya then Lesser Himalaya and finally Sub-Himalayan sequences which correspond

the southward sequence of thrust development in the Himalayan orogenic belt. The model also shows that the frontal part of the Himalayas is more vulnerable to develop fault suggesting the active nature of the regime. This is consistent with the characteristics of neotectonics based on the active fault studies in the Himalayas. The Himalayan front is the most active fault zone of the Himalayas (Nakata, 1989; Thakur et al., 2000). Thus, the predicted thrust fault is the important tectonic features related to the present Himalayan collision. Furthermore, The successive development of fault from Late Eocene to present shows the close relation with the transformation of active subduction of Indian continental crust in the Himalayas during the post-collisional period (Johnson, 2002).

Plate convergence and southward thrust propagation

It is well known that the Himalayas were created as a result of collision of the northward moving Indian continent with the Asian landmass. That orogenic process continues, and mountains are still being formed. The continued activity is manifested in the present day northward movement of India at a rate of about ~2 cm/a and in occurrence of frequent seismic events along the mountain range and it's surroundings (Seeber et al., 1981; Pandey et al., 1995). Most of the convergence is accommodated within the Himalayas by the movements on various faults and thrusts (Upreti, 1999); as a result the basic framework or architecture of the Himalaya is controlled by these major thrusts. The master thrusts of Himalaya are MCT, MBT and MFT which extend all along the Himalayan range. The three thrusts are considered to come together in a low angle decolement known as the MHT to the north, depth varies below the different sub-divisions of Himalayas. The decollement is major crustal break separating the upper and lower continental crust of the Indian plate. The lower crust underthrusts to the north below the Tibetan continental crust resulting in the doubling the crust below the Tibet but the crust above the decollement is being pushed out to the south along these three master thrusts. The initiation of these thrusts was younger in the age from north to south (DeCelles et al., 2001). The MCT was the first thrust to break the Indian crust (Schelling, 1992). It carried southward on its back a pile of rocks 25-30 km thick for 200 km or more. Gradually the second and third major intracontinental thrusts were formed southwardly in different time being (Upreti, 1999). Thus, these sceneries suggest that the MCT is the most oldest and MFT is the youngest thrusts in the Himalayas which propagate southward from their initiation time. From the present simulation, we observed almost the same tendency of thrust faults formation in all models. In order to examine the tendency of faults development and their propagation, we performed a number of experiments adopting various convergent displacement boundary conditions (up to 2000 m), which clear the successive formation of thrust faults in the Tethys Himalaya, Higher Himalaya, Lesser Himalaya and Sub-Himalaya. All experiments predict faulting to develop in the north in Tethys and Higher Himalaya at 40 Ma then to propagate in the more southern part in the lesser Himalaya at 20-10 Ma and finally to the most southern part

Sub-Himalaya. These sceneries mimic the sequence of southward thrust development in the Himalayan orogenic belt after collision. Therefore, the formation of successive thrusts and their southward propagation might be due to the continuous convergence effects of Indian sub-plate under the Eurasian plate.

Incipient zones and early development state of MCT, MBT and MFT

The continuing northward compressional movement of India has produced intracontinental thrusts (Le Fort, 1975; England and Molnar, 1993). The major thrusts are the MCT, MBT and MFT in Himalayas which are produced by the continual northward compressional movement of Indian sub-plate (Upreti, 1999). Howfar, there are many hypotheses have been proposed to clarify the development history of the Himalayan major thrusts but this topic is still highly controversial. In the present numerical modeling, we examined the early development state of these thrusts based on hypothesis of Lyon-Caen and Molnar (1983) and Johnson (2002). In order to state this hypothesis, they proposed a series of balanced geologic profiles on the different structural development stage of Himalayas where indicated that the MCT, MBT and MFT were initially created from the incipient development zones at 40, 20 and 10 Ma, besides their formation ware completed at 20, 10 and 0 Ma, respectively. In these balanced profiles, they marked the early developing state of future thrusts by dashed line and mature stage by solid line (Fig. 7). Therefore, these early to mature stage boundaries are defined in terms of incipient development zones of such thrusts for the present modeling. The geometrical position of MCT and MBT zones are below the Hihger Himalaya which are equivalent to the lesser Himalayan sequences. The position of MFT zone is the southern part of lesser Himalaya and equivalent to Sub-Himalaya. Thus the meta-sedimentary and clastic sedimentary rocks are considered for those zones, respectively. After selecting these geometries and rheological properties, the finite element method with Mohr's coulomb criterion has been applied to calculate the early development stages stress state and faults. Calculation shows that whole area of such zones covered by compressive stress and thrust faults. We also examined the differential stress and maximum shearing stress in the models and values of these stresses are comparatively high in these zones (Fig. 13). Thus from the intensities of stress values and high concentration of thrust faults in these early developing zones, it can be postulate that the major thrust might be created primarily from these zones, where the probable principal thrusting mechanisms were: (a) primarily a broad blind share-band was formed which was continuously perturbed by compressional movement as a result the future thrusts were developed with time beings; (b) the large number of small-scale thrust faults were formed within the incipient zones which probably influenced to form these large scale major thrusts in the respective time; (c) the horizontal direction of maximum compressional stress component along or the elongation of initial incipient boundaries may be one of the important cause to develop these thrusts, or (d) all of these above mentioned mechanisms were influential to attribute such

structures.

Tectonic synthesis of simulated structures after collision

Today our understanding of the geology and tectonics of the Himalayas have greatly advanced. It was built over works of a large number of geologists for over one and half centuries. As a result, Himalayas perhaps geologically the most well know part of the world. Intensive studies were made here on the problems of the inverted metamorphism, tectono-thermal evolutionary history, magmatism, foreland basin development and seismotectonics and so on. Despite these advances in the Himalayan geology, a great deal of uncertainties still exists regarding the tectonic development, origin of the inverted metamorphism and the tectono-thermal evolution of the Himalayas. A variety of models have been postulated for explaining the structural development and tectonics in the Himalayas (Molnar and Tappornnier, 1975; Seeber et al., 1981; Lyon- Caen and Molnar, 1983; England and Thompson, 1984; Hubbard 1986; Chemenda et al., 1995; Kaneko, 1995 &1997; Upreti, 1999; Chemenda et al., 2000; Yin and Harrison, 2000; Johnson, 2002). The first post-collisional evidence of crustal thickening is thin-skinned thrusting in the Tethyan Himalaya, Eo-Himalayan metamorphism, and deformation in the north Tibet. The later, initiated between 45-32 Ma. At 31 ± 1 Ma, crustal thickening began in south Tibet along the thrust, moving southward to the Himalaya shortly thereafter in a series of S-directed thrusts (MCT, MBT, MFT) that sole into a common decollement (DeCelles et al., 2001).

Meanwhile, the principal thrusts MCT, MBT and MFT show shallowing depth towards south, suggesting southward migration of the main deformation front. Neotectonic activity and active faulting related to the thrusts are observed on the surface in some restricted segments. The MCT remains largely inactive, except some reactivated segments showing lateral strike-slip movement as in central Nepal. The MBT in certain localized areas exhibits neotectonic activity (Nakata, 1989). The MFT shows active faulting and associated uplift. The MFT represents a zone of active deformation between the Sub-Himalaya and the Indian gangetic plain, which demarcates the present day principal tectonic displacement zone between the stable Indian continent and the Himalayas with a convergence rate of 20 mm/a (Lave and Avouac, 2000). Active faulting is observed along the MBT and MFT in the Himalayan front of southeast Nepal. The river terraces along the MBT show both vertical and horizontal displacements (Mugnier et al., 1992). In the present studies, we simulated the thrust faults appealing the successive convergent displacement derived (2000 m for model A, 1000 m for model B and C and 400 m for D) from convergent rate and layers properties after collision. The results of the simulated models A, B and C show Indian continental crust as well as the incipient zones of MCT (40-20 Ma), MBT (20-10 Ma) and MFT (10-0 Ma) are very sensitive to form thrust faults in respective geologic age. These results corresponded with the structural evolutionary models of Chemenda et al. (1995) and Chemenda et al. (2000).

Chemenda et al. (1995) and Chemenda et al. (2000) reported that the force full high compression during 20-35 Ma leading to failure occur in front of subduction zone and formed the Main central Thrust. Compression then gradually decreased and underthrusting continued along the MCT until the formation of next major thrust MBT at 10 Ma and finally the MFT formed under the low compression in the younger sequence. Moreover large number of thrust faults within the incipient zones of major thrusts as well as the initial boundaries of such future thrusts which are also an evidences to the earlier development state of the major thrusts. Still, the interpretation of numerical results remains somewhat ambiguous because of the limitation of elastic modeling. Despite these limitations, modeling results are comparable with the previous data. Combining these simulated results with previous data, we presented a hypothetical model on the development stages of different major geologic structures of Himalayas are shown in Fig. 20. It is well known that the tectonics and structures of Himalayas are directly related to the characteristics of the major thrust from the very early to present collision. We used also present profile which commonly revel that the faults are intensely concentrated along the elongation of real MBT and MFT, suggesting that this area (frontal) might be active which is consistent with the present day neotectonic activity in the Himalaya. From these observations, it is cleared that the nature of structures and tectonics of Himalayas are the primary basis of MCT, MBT and MFT with their associated small-scale faults. Moreover, the successive development of simulated trust faults is the direct supporting evidences to the transformation active subduction in the Himalayas from the early post collision time to present. The active subduction in the Himalayas has been transferred from the Tsangbo suture to first 50 Ma to thrust within the Tethyan sequence, then to the MCT (20-25 Ma), then to the MBT (10 Ma) and finally to the MFT (>0 Ma) at present (Lyon- Caen and Molnar, 1983; Johnson, 2002).

Conclusions

A series of 2D plane strain finite element models with Mohr-Coulomb failure criterion have been presented to simulate the stress state and thrust faults within the brittle upper crust for understanding the tectonics of the Himalayan mountain ranges. The Himalaya is the most significant mountain chain on earth providing a spectacular natural laboratory for the study of continental collision in the uplifted section of crust. For these reasons, the numerical study was performed on the geologic profiles of central Nepal Himalaya considering the convergent displacement that is subjected along the SW-NE horizontal direction and rock layer properties in the regime. Primarily, the results of the simulated models are compared with the available geologic, seismic and earthquakes focal mechanism solution data of the region and finally concluded the development of thrust faults and their associated tectonics in the Himalayas.

1. Finite element modeling state of stresses is compressive pattern which supports the continuous NS compressional influences of Indian plate to the Himalayan profiles where maximum principal stress oriented horizontally, is resulting the thrust faults of the models.
2. The convergent displacement and rock layers properties of models are primarily controlled the nature of stress and fault. Modeling results detect that the changing boundary displacements are sensitive for both of the of stresses magnitude and faults whereas layer properties are mainly sensitive to the fault development and very slightly to the stress field, indicating that the model displacement boundary conditions play more important roles than the difference of layer properties.
3. It is observed that the thrust faults are frequently localized within the low-grade rocks layers of the younger profile than the high-grade rock layers of older profiles. Thus the formation of fault is more vulnerable in the low-grade rock layers than the high-grade rock layers of the regime for all stages of models.
4. The thrust faults are developed by adopting the layer properties in the present models, are corresponded with field fault data as well as the natural states of faults in the Himalayas. Different fault studies reported that there are many thrust faults distributed in the Himalayas since middle Tertiary to present. Thus the adopted ranges of layer properties are suitable for the elastic finite element simulation.
5. Faulting tendency in the models increase towards shallow depth and south. In the north, where detachment is deep, and rock strength is great, showing very few failure elements (faults) besides in the south, where detachment is shallower, and the rock strength is weaker, foreland strata are highly deformed by faulting above shallower dipping detachment. The results mimic the structures in the frontal part of Himalayas, where imbricate thrusting is common.
6. Numerical models predict thrust faulting to develop in the north inTibetan oceanic crust, Tethys and Higher Himalaya at 40 Ma then to propagate in the more southern part in the lesser Himalaya at 20-10 Ma and finally to the most southern part Sub-Himalaya in the younger rock sequences. These sceneries mimic the sequence of southward thrust development in the Himalayan orogenic belt after collision. These results also suggest that the MCT might be the oldest and MFT is the youngest thrust in the Himalayas.
7. The thrust faults appeared in the Indian continental crust as well as the incipient zones of MCT (40-20 Ma), MBT (20-10 Ma) and MFT (10-0 Ma) with high convergent displacement 2000 m in model A, than decreased 1000 m in model B and C and 400 m in D. These results support the convergence rate stated in the structural evolutionary models of Chemenda et al. (2000). Therefore, the imposed convergent displacement boundary conditions are well fit with the developing situation of major thrusts.

8. The major thrusts are the MCT, MBT and MFT in Himalayas which are produced by the continual northward compressional movement of Indian sub-plate. The MCT, MBT and MFT were created at 40, 20 and 10 Ma, whereas their formation was completed at 20, 10 and 0 Ma, respectively. Present simulation shows that the thrust faults are uniformly concentrated within the incipient zones as well as the incipient boundaries of such thrusts, which must have been responsible for the early development of these thrusts.
9. Simulated thrust faults in the Tethys Himalaya and Higher Himalaya at 40-20 Ma then Lesser Himalaya at 10 Ma and finally in the Sub-Himalayan sequence at present stage indicating that primarily subduction zone was in the Tethys Himalaya and with continuous convergence of Indian Sub-Plate, It transformed to the Higher, Lesser and finally in Sub-Himalayan region.
10. Moreover, the models also show that the frontal part of the Himalayas is more vulnerable to develop faults suggesting the active nature of the regime. This is consistent with the characteristics of neotectonics based on the active fault studies in the Himalayas. The Himalayan front is the most active fault zone in the Himalaya (Nakata, 1989).

Finally, the results of numerical simulation models allow us to conclude that the successive convergent rate leads to form Himalayan thrusts within the Indian continental crust and intensities of thrust development within the incipient zones of the major thrusts imply that these zones might be the primary zones for developing the MCT, MBT and MFT where age of the initiation of these thrusts become younger from north to south, with the MCT as the oldest and the MFT as the youngest which suggesting their propagation from north to south. We believe that these thrusts propagation might be due to the continuous convergent activity of Indian plate which directly influenced the tectonics and structures in the regime. Moreover the intense distribution of deformation pattern around the major thrusts and along the frontal part of Himalaya indicating that these areas are tectonically active. It refers that this activity is the most important tectonic features associated with present neotectonics in the Himalayas.

Acknowledgement

MFH is grateful to Ministry of Education, Culture, Sports, Science and Technology, Japan for financial support that made this study possible and he is also grateful to Heiwa Nakajima scholarship Foundation, Tokyo, Japan.

References

Anderson, E. M., 1951, The dynamics of faulting and dyke formation with applications to

Britain, 206 pp., 1st ed., Edinburgh.

Arita, K., 1983. Origin of the inverted metamorphism of the lower Himalayas, central Nepal. *Tectonophysics*, 95, 43-60.

Arita, K., Shiraishi, K. and Hayashi, D., 1984. Geology of western Nepal and a comparison with Kumaun, India. Jour. Fac., Sci., Hokkaido Univ., Ser. IV., 21(1), 1-20.

Armbuster, J., Seeber, L. and Jacob, K. H., 1978. The northwestern termination of the Himalayan mountain front: Active tectonics from microearthquakes. *J. Geophys. Res.* 83, 269-282.

Armijo, R., Tapponnier, P., Mercier, J. L. and Tonglin, H., 1986. Quaternary extension in southern Tibet. Journal of Geophysical Research, 91, 13,803-13,812.

Bilham, R., Larson, K., Freymueller, J., and Project Idylhim members, 1997. GPS measurements of present-day convergence across the Nepal Himalaya. *Nature*, 386, 61-64.

Blisniuk, P., Hacker, B.R., Glodny, J., Ratschbacher, J., Bi, S., Wu, Z., Mcwilliams, M.O. and Calvert, A. 2001. Normal faulting in central Tibet since at least 13.5 Ma ago. *Nature*, 412, 628-632.

Bott, M.H.P., 1990. Stress distribution and plate boundary force associated with collision mountain ranges, *Tectonophysics*, 182, 193-209.

Burchfiel, B. C., Zhiliang, C., Hodges, K. V., Yunping, L., Royden, L. H., Changrong, D, and Jiene, X., 1992. The south Tibet detachment system, Himalayan orogen : Extension contemporaneous with and parallel to shortening in a collisional mountain belt. *Geol. Soc. Amer., Spec, Pub.*, 269, 41.

Burg, J. P. and Chen, G. M., 1984. Tectonics and structural zonation of southern Tibet, China. *Nature*, 311, 219-223.

Chamlagain, D. and Hayashi, D., 2004. Numerical simulation of fault development along NE-SW Himalayan profiles in Nepal, *J. Nepal Geo. Soc.*, 29, 2004.

Chandra, U., 1978. Seismicity, Earthquake Mechanisms and tectonics along the Himalayan mountain range and vicinity. *Phys. Earth Planet. Inter.*, 16, 109-131.

Cattin, R. and Avouac, J. P., 2000. Modeling mountain building and the seismic cycle in the Himalaya of Nepal. *Jour. Geophys. Res.* 105 (B6), 13,389-13,407.

Chemenda, A., Burg, J.P. and Mattauer, M. 2000. Evolutionary Model of the Himalaya-Tibet System: Geopoem Based on New Modeling, Geological and Geophysical Data. *Earth Planet. Sci. Lett.*, 174, 397-409.

Chemenda, A., Mattauer, M., Malavieille, J. and Bokun, A.N., 1995. A mechanism of syn-collisional deep rock exhumation and associated normal faulting: results from physical modeling. *Earth Planet. Sci. Lett.*, 132, 225-232.

Cloetingh, S. and Wortel, R., 1986. Stress in the Indo-Australian plate. *Tectonophysics*, 132, 49-67.

Dèzes, P., 1999. Tectonic and Metamorphic Evolution of the Central Himalayan Domain in

Southeast Zanskar (Kashmir, India). Memoires de Gèologie (Lausanne), 32, 1015-3578.

DeCelles, P.G., Robinson, D.M., Quade, J., Copeland, P., Upreti, B.N., Ojha, T.P. and Garzione, C.N., 2001. Regional structure and stratigraphy of the Himalayan fold-thrust belt, far western Nepal. *Tectonics*, 20, 487-509.

England, P.C. and Thompson, A.B., 1984. Pressure-temperature-time paths of regional metamorphism, part 1: Heat transferring the evolution of regions of the thickened continental crust. Jour., Petrol., 25, 929-954.

England, P. and Molnar, P., 1993. The interpretation of inverted metamorphic isograds using simple physical calculations, *Tectonics*, 12, 145-157.

Fuchs, G. and Frank, W., 1970. The geology of west Nepal between the rivers Kali Gandaki and Thulo Bheri. *Jahrb. Bundesanst. Sonderb.* 18, 1-103.

Fuchs, G. and Linner, M., 1995. Geological traverse across the western Himalaya-A contribution to the geology of eastern Ladakh, Lahul and Chamba. *Geol. Bundesanst,* 138(4), 655-685.

Gansser, A., 1964. Geology of the Himalayas: London, Wiley Inter. Science, 289p.

Gerbault, M., Alexei, N., Poliakov, B. and Daignieres, M., 1998. Prediction of faulting from the theories of elasticity and plasticity: what are the limits. *J. Structural Geology*, 20, 301-320.

Hagen, T., 1969. Report on the geological survey of Nepal. Denkschr. Schweiz. Natur. Gesell., 86(1), 1-185.

Harrison, T.M., Grove, M., Lovera, O.M. and Catlos, E.J., 1998. A model for the origin of Himalayan anatexis and inverted metamorphism. *J. Geophys. Res.*, 103, 27017-27032.

Hassani, R., Jongmans, D. and Chery, J., 1997. Study of the plate deformation and Stress in subduction processes using two-dimensional numerical models, Jour. Geophys. Res., 102 (B8), 17951-17965.

Hashimoto, S., et al., 1973. Geology of Nepal Himalayas, *Saikon, Tokyo, 286p.*

Hayashi, D., 1987. Numerical simulation of the uplift of the Tibetan Plateau. *Jour. Geol. Soc. Jap.*, 93, 587-595.

Hayashi, D., 2002. Unpublished software.

Hayashi, D., Fuji, Y., Yoneshiro, T. and Kizaki, K., 1984. Geology of Karnali-Bheri region, west Nepal. *Jour. Nepal Geol. Soc.*, 2, 29-40.

Hayashi, D. and Kizaki, K., 1972. Numerical analysis on migmatite dome with special reference to finite element method. *J. Geol. Soc. of Japan*, 78, 677-686.

Hodges, K.V., Parrish, R. R. and Searle, M. P., 1996. Tectonic evolution of the central Annapurna Range, Nepalese Himalayas. *Tectonics*, 15, 1264-1291.

Howladar, M. F. and Hayashi, D., 2003. Numerical fault simulation in the Himalaya with 2 D finite element method. J. Polar Geoscience, 16, 243-258.

Howladar, M. F. and Hayashi, D., 2004. Simulation of Himalayan major thrusts by finite element method. *J. Geoinformatics, 15(4), 207-219.*

Hubbard, M.S., 1996. Ductile shear as a cause of inverted metamorphism: example from the Nepal Himalaya. Geol., 104, 493-499.

Jacob, K. H., Armbuster, J., Seeber, L. and Pennington, W., 1976. Tarbela reservoir: A region of compressional tectonics with reduced seism city upon initial reservoir filling. first Int. Symp. In induced seism city (ISIS), Banff, Canada, Engineering Geology.

Johnson, M. R.W., 2002. Shortening budgets and the role of continental subduction during the India-Asia collision. *Earth-Science Reviews*, 59, 101-123.

Joshi, A. and Patel, R.C., 1997. Modeling of active lineaments for predicting a possible earthquake scenario around Dehradun, Garhwal Himalaya, India. Tectonophysics, 283, 289-310.

Kaneko, Y., 1995. Thermal structure in the Annapurana region, central Nepal Himalaya: implication for the inverted metamorphism. Jour. Mineral. Petrol. Econ. Geol., 90, 143-154.

Kaneko, Y., 1997. Two-step exhumation model of the Himalayan metamorphic Belt, central Nepal. Jour. Geol. Soc. Jap., 103(3), 203-226.

Kano, T., 1984. Geology and structure of the Main Central Thrust zone of the Annapurana range, Central Nepal Himalayas. *J. Geol. Soc. Japan*, 2, 31-50.

Kizaki, K. and Hayashi, D., 1984. Geological Map of Nepal, unpublished.

Lave, J. and Avouac, J. P., 2000. Active folding of fluvial terraces across the Siwaliks Hills, Himalayas of central Nepal. *Journal of Geophysical Research*, 105, 5735-5770.

Lyon-Caen, H. and Molnar, P., 1983. Constraints on the structure of the Himalaya from an analysis of gravity anomalies and a flexural model of the lithosphere. *Journal of Geophysical Research*, 8, B10, 8171-8191.

Le Fort, P., 1975. Himalayas: the collide range, present knowledge of the continental arc. American Jour. Sci., 275, 1-44.

Le Fort, P., 1996. Evolution of the Himalaya, in The Tectonic Evolution of Asia, edited by A. Yin and T.M. Harrison, Cambridge University Press, New York, 95-109.

Le Pichon, X., Fournier, M. and Jolivet, J., 1992. Kinematics, topography, shortening and extrusion in the India-Asia collision. *Tectonics*, 11, 1085-1089.

Meigs, A. J., Burbank, D.W. and Beck, R. A., 1995. Middle-late Miocene [>10 Ma] formation of the Main Boundary Thrust in the Western Himalaya. Geology, 23, 423-426.

Melosh, H. J. and Williams, C. A., 1989. Mechanics of Graben formation in crustal rocks: a Finite element analysis. *J. Geophys. Res.*, 94, 13961-13973.

Minster, J. B. and Jordan, T. H., 1978. Present day plate motions. *J. Geophys. Res.*, 83, 5331-5354.

Molnar, P., 1990. A review of the rates of active understanding and deformation at the Himalaya. *J. Him. Geol.* 1, 131-154.

Molnar, P., Fitch, T. J., Wu, F. T., Chen, W. P., Warsi, W. E. K. and Tapponnier, P.,

1977.

Structure and tectonics of Himalaya: A brief summary of relevant geophysical observations. Himalaya, *Science de la Terre, Center National de la Recherche Scientique, Paris*, 269-294.

Molnar, P. and Tapponnier, P., 1975. Cenozoic tectonics of Asia: effects of continental collision. Science, 189, 419-426.

Molnar, P. and Tapponnier, P., 1978. Active tectonics of Tibet. *J. Geophys. Res.*, 83, 5361-5375.

Mugnier, J. L., Mascle, G. and Faucher, T., 1992. La structure des Siwaliks de Iouest du Nepal: Un prisme d'accretion intracontinental. Bull. Soc. Geol. Fr., 163., 585-595.

Nakata, T., Iwata, S., Yamanaka, H., Yagi, H. and Maemoku, H., 1984. Tectonic landforms of several active faults in the western Nepal Himalayas. *J. of Nepal Geological Society*, 4, 177-200.

Nakata, T., 1989. Active faults of the Himalaya of India and Nepal. Special paper *Geological Society of America*, 232, 243-264.

Nakata, T., Otsuki, K. and Khan, S. M., 1990. Active faults, stress field and plate motion along the Indo-Eurasian plate boundary. *Tectonophysics*, 181, 83-95.

Ni, J. and Barazangi, M., 1984. Seismotectonics of the Himalayan collision zone; geometry of the underthrusting Indian plate beneath the Himaya. J. Geophys. Res., 89, 1147-1163.

Pandey, M. R., Tandukar, R. P., Avouac, J. P., Lave, J. and Massot, J.P., 1995. Interseismic strain accumulation on the Himalayan crustal ramp (Nepal). *J. Geophysical Research Letter*, 22, 751-754.

Patriat, P. and Achache, J., 1984. India-Eurasia collision chronology has implications for crustal shortening and driving mechanism of plates. *Nature*, 311, 615-621.

Sakai, H., 1985. Geology of the Kali Gandaki Supergroup of the lesser Himalaya in Nepal. *Mem. Fac. Sci. Kyushu Univ., Ser. D. Geol.*, 25, 337-397.

Sato, K., Bhatia, S. C. and Gupta, H. K., 1996. Three-dimensional numerical modeling of deformation and stress in the Himalaya and Tibetan Plateau with a simple geometry, *J. Phys. Earth.*,44, 227-254.

Schelling, D., 1992. The tectonostratigraphy and structure of the eastern Nepal Himalaya. *Tectonics*, 11, 925-943.

Schelling, D. and Arita, K., 1991. Thrust tectonics, crustal shorteningand structure of the far eastern Nepal Himalaya. *Tectonics*, 10, 851-862.

Searle, M. P., 1983a. Stratigraphy, structure and evolution of the Tribetan-Tethys zones in Zanskar and the Indus suture zone in the Ladakh Himalaya. Royal Society of Edinburg Transactions, *Earth Sciences*, 73, 205-219.

Searle, M. P., 1986. Structural evolution and sequence of thrust in the Higher Himalaya, Tibetan-Tethys and Indus suture zone of Zanskar and Ladakh, western Himalaya.

Jour. of structural Geology, 8, 923-936.

Searle, M. P., Windley, B. F., Coward, D. J. W., Rex, A. J., Rex, D., Tindong Li, Xuchang, X., Jan, M. Q., Thakur, V. C. and Kumar, S., 1987. The closing of Tethys and the tectonics of the Himalaya. *Geological Society Bulletin of America,* 98, 678-701.

Seeber, L., Armbuster, J. G. and Quittmeyer, R. C., 1981. Seismicity and continental subduction in the Himalayan Arc. *Geodynamic series,* 3, 215-242.

Seeber, L. and Gornitz, V., 1983. River profiles along the Himalayan arc as indicators of active tectonics, *Tectonophysics,* 92, 335-367.

Shanker, D., Kapur, N. and Shing, B., 2002. Thrust-wedge mechanics and coeval development of normal and reverse faults in the Himalayas. *Jour. Geol. Soc. London,* 159, 273-280.

Sinha, A.K., 1987. Tectonic zonation of the central Himalayas and the crustal evolution of collision and compressional belts. *Tectonophysics,* 134, 59-74.

Sibson, R.H., 1994. Crustal stress, faulting and fluid flow. Geofluids: origin, migration, and evolution of fluids in sedimentary basins, *Special publication of Geol. Soc. London,* 54, 15-28.

Sorkhabi, R. B. and Macfarlane, A., 1999. Himalaya and Tibet: Mountain roots to mountain tops, in Macfarlane, A., Sorkhabi, R.B, and Quade, J., eds., Himalaya and Tibet: Mountain Roots to Mountain Tops. *Geol. Survey of America,* 328, 1-8.

Spikantia, S.V., 1987. Himalaya - the collided orogen: a plate tectonic evolution on geological evidences. *Tectophysics,* 134, 75-90.

Thakur, 2004. Active tectonics of Himalayan Frontal Thrust and Seismic Hazard to Ganga Plain. *Current Science,* 86,1554-1560.

Thakur, V.C., Sriram, V. and Mundepi, A.K., 2000. Seismotectonics of the great 1905 Kangra earthquake meizoseismal region in Kangra-Chamba, NW Himalaya. *Tectonophysics,* 326, 289-298.

Tapponnier, R., et al., 1990. The Ailo Shan/Red river metamorphic belt: Tertiary left lateral shear between Indo-China and south China. *Nature,* 343, 431-437.

Timoshenko, S. P. and Goodier, J. N., 1970. Theory of elasticity, edited by McGraw-Hill, 567pp., London press, 3rd ed.

Trelor, P. J., Coward, M. P., Chambers, A. F., Izatt, C. N. and Jackson, K. C., 1992. Thrust geometries, interferences and rotations in the Northwest Himalaya. *Thrust Tectonics,* edited by McClay, 325-342.

Turcotte, D. L. and Schubart, G., 1982. Geodynamics: Applications of Continuum Physics to Geological problems. *John Wiley and Sons,* 450p.

Upreti, B. N., 1999. An overview of the stratigraphy and tectonics of the Nepal Himalaya. *J. Asian Earth Sci.,* 17, 577-606.

Verma, R.K., 1997. Paleomagnetism from Parts of Tethys Himalaya, Indus Suture Zone, Ladakh and South Tibet: Implications for Collision between Indian and Eurasian

Plate. *J. Himalayan Geology*, 18, 93-102.

Windley, B.F., 1989. Metamorphism and tectonics of the Himalayas, *Journal of Geological of Society of London*, 140, 849-866.

Windley, B.F., 1995. The Evolving Continents, *3rd Edition, John Wiley & Sons*: Chichester, 526 p.

Yeats and Lillie, 1991. Contemporary tectonics of Himalayan frontal fault system: folds, blind thrust and the 1905 Kangra earthquake. *J. Structural Geology*, 13, 215-225.

Yin, A., Harrison, T. M., Ryerson, F. J., Wenji, C., Kidd, W. S.F., and Copeland, P., 1994. Tertiary structural evolution of the Gangdese Thrust system, southeastern Tibet, *J. Geophys. Res.*, 99, 18175-18201.

Yin, A. and Harrison T M., 2000. Geologic evolution of the Himalayan-Tibetan orogen, *Annual reviews of Earth and Planetary Sciences*, 28, 211-280.